

AD-A084 643

SCIENCE APPLICATIONS INC MCLEAN VA
MX MPS DEPLOYMENT, AN ON-SITE FALLOUT EVALUATION, (U)
DEC 78 R H CRAVER, J T MCGAHAN, E MULLER
SAI-79-866-WA DNA-4813F

F/G 18/8

DNA001-78-C-0350

UNCLASSIFIED

ML

1 OF 1
40 -
AD84643

END
DATE
FILMED
6-80
DTIC

ADA 084643

LEVEL III

AP-E 300 773

12

✓ DNA 4813F

MX MPS DEPLOYMENT

An On-Site Fallout Evaluation

R. H. Craver
J. T. McGahan
E. Muller
Science Applications, Inc.
8400 Westpark Drive
McLean, Virginia 22102

29 December 1978

Final Report for Period 12 July 1978—29 December 1978

CONTRACT No. DNA 001-78-C-0350

APPROVED FOR PUBLIC RELEASE;
DISTRIBUTION UNLIMITED.

THIS WORK SPONSORED BY THE DEFENSE NUCLEAR AGENCY
UNDER RDT&E RMSS CODE B325078464 Q99QAXNA01110 H2590D.

Prepared for
Director
DEFENSE NUCLEAR AGENCY
Washington, D. C. 20305

DTIC
ELECTE
S MAY 23 1980 D
D

80 4 28 125

Destroy this report when it is no longer needed. Do not return to sender.

PLEASE NOTIFY THE DEFENSE NUCLEAR AGENCY,
ATTN: STTI, WASHINGTON, D.C. 20305, IF
YOUR ADDRESS IS INCORRECT, IF YOU WISH TO
BE DELETED FROM THE DISTRIBUTION LIST, OR
IF THE ADDRESSEE IS NO LONGER EMPLOYED BY
YOUR ORGANIZATION.



UNCLASSIFIED

SECURITY CLASSIFICATION OF THIS PAGE (When Data Entered)

REPORT DOCUMENTATION PAGE		READ INSTRUCTIONS BEFORE COMPLETING FORM
1. REPORT NUMBER DNA 4813F	2. GOVT ACCESSION NO. ✓ AD-A084643	3. RECIPIENT'S CATALOG NUMBER
4. TITLE (and Subtitle) MX MPS DEPLOYMENT An On-Site Fallout Evaluation		5. TYPE OF REPORT & PERIOD COVERED Final Report for Period 12 Jul 78—29 Dec 78
		6. PERFORMING ORG. REPORT NUMBER SAI-79-866-WA ✓
7. AUTHOR(s) R. H. Craver J. T. McGahan E. Muller		8. CONTRACT OR GRANT NUMBER(s) DNA 001-78-C-0350 <i>JWW</i>
9. PERFORMING ORGANIZATION NAME AND ADDRESS Science Applications, Inc. ✓ 8400 Westpark Drive McLean, Virginia 22102		10. PROGRAM ELEMENT, PROJECT, TASK AREA & WORK UNIT NUMBERS Subtask Q99QAXNA011-10
11. CONTROLLING OFFICE NAME AND ADDRESS Director Defense Nuclear Agency Washington, D.C. 20305		12. REPORT DATE 29 December 1978
14. MONITORING AGENCY NAME & ADDRESS (if different from Controlling Office)		13. NUMBER OF PAGES 78
		15. SECURITY CLASS (of this report) UNCLASSIFIED
16. DISTRIBUTION STATEMENT (of this Report) Approved for public release; distribution unlimited.		15a. DECLASSIFICATION DOWNGRADING SCHEDULE
17. DISTRIBUTION STATEMENT (of the abstract entered in Block 20, if different from Report)		
18. SUPPLEMENTARY NOTES This work sponsored by the Defense Nuclear Agency under RDT&E RMSS Code B325078464 Q99QAXNA01110 H2590D.		
19. KEY WORDS (Continue on reverse side if necessary and identify by block number)		
Fallout Hazard	MX Multiple Protective Structure Deployment	
Monitor Points	Hypothetical Massive Attack	
Wind Samples	On-Site Doses and Dose Rates	
Entry Times	Transmission Factors	
Feasibility	Equipment and Personnel Vulnerability	
20. ABSTRACT (Continue on reverse side if necessary and identify by block number)		
This report addresses the probable extent and severity of the fallout hazard associated with a massive hypothetical attack against an MPS Deployment of the MX missile in the Nevada Model Area. It contains descriptions of attack scenarios, site modeling, methodology for calculating and depicting the distribution of fallout, and quantitative estimates of the severity of the hazard.		

DD FORM 1473

1 JAN 73

EDITION OF 1 NOV 65 IS OBSOLETE

UNCLASSIFIED

SECURITY CLASSIFICATION OF THIS PAGE (When Data Entered)

UNCLASSIFIED

SECURITY CLASSIFICATION OF THIS PAGE(When Data Entered)

20. ABSTRACT (Continued)

Forty separate wind samples taken over a twelve-month period are used to assess the variability of the distribution of fallout resulting from an attack of several thousand surface burst weapons at the Nevada site. Fallout intensities are determined at 177 monitor points throughout the potential deployment area; time histories of dose rate buildup and decay are presented and discussed with respect to operational implications. Key factors are parameterized to permit comparison of a range of design factors and logistical considerations.

Key findings are presented in condensed form including several illustrative examples chosen to quantify the practical aspects of operating in a radiation environment and to assist in the development of a balanced system design.

Accession For	
NTIS GRA&I	<input checked="" type="checkbox"/>
DDC TAB	<input type="checkbox"/>
Unannounced	<input type="checkbox"/>
Justification	<input type="checkbox"/>
By _____	
Distribution/	
Availability Codes	
Dist.	Avail and/or special
A	

DTIC
ELECTE
MAY 23 1980
S D D

UNCLASSIFIED

SECURITY CLASSIFICATION OF THIS PAGE(When Data Entered)

PREFACE

This study was sponsored by the Defense Nuclear Agency, under Project V99QAXN, Task Area A011, Work Units 01 and 10, "On Site Fallout Evaluation." The work was sponsored by Science Applications, Incorporated under DNA Contract 001-78-C-0350. The contract monitor was Dr. David L. Auton of DNA. Data used in the report were developed primarily by SAI during the course of the study except for certain parameters pertaining to deployment areas, patterns and attack scenarios which were provided by the U.S. Air Force Systems Command Space and Missile Systems Organization (SAMSO).

TABLE OF CONTENTS

<u>Section</u>	<u>Page</u>
PREFACE	1
1 INTRODUCTION	7
1.1 PROBLEM	7
1.1.1 Bounding the Problem	7
1.1.2 Refinements.	8
1.2 OFFENSIVE THREAT.	8
1.3 ASSUMPTIONS	8
1.4 FINDINGS.	8
1.4.1 Illustrative Problems.	9
1.4.2 Implications	11
1.4.3 Summation.	12
2 SITE MODELING AND SCENARIO PARAMETERS.	15
2.1 THE DEPLOYMENT AREA	15
2.2 THE CONCEPT	15
2.3 MODELING DEPLOYMENT CONFIGURATION	17
2.4 ATTACK SCENARIOS.	19
3 METHODOLOGY.	21
3.1 CONCEPTS.	21
3.1.1 Approach to the Multi-Burst Problem.	21
3.1.2 Treatment of Assumptions	21
3.1.3 Program Development.	22
3.1.4 Equivalent Dose Rate Configurations.	23
3.1.5 Mathematical Formulation	24
3.1.6 Field Definition	24
3.1.7 Modifications to DELFIC.	25
3.1.8 Computation of Fallout at a Point.	26
3.1.9 Comments on the Methodology.	27
3.1.10 Determination of Dose Rate Time Dependency	27
3.1.11 Determination of Percent Activity On Site.	28
3.1.12 DELFIC Input Parameters.	28
3.1.13 DELFIC Fallout Field Computation	29
3.1.14 Wind Profile Data.	31
4 POTENTIAL INTERACTIVE EFFECTS.	41
4.1 EARLY TIME MULTIBURST DUST CLOUDS	41
4.2 STATUS OF MULTIPLE BURST INVESTIGATIONS RELATED TO MX	46

TABLE OF CONTENTS (continued)

<u>Section</u>		<u>Page</u>
5	RESULTS	51
	5.1 TYPICAL RADIATION LEVELS	51
	5.2 IMPACT OF WIND VARIATION	51
	5.3 ACTIVITY AND MASS DEPOSITED ON SITE	52
	5.4 OPERATIONAL IMPLICATIONS	53
	5.5 RADIATION ARRIVAL TIMES AND PERSISTENCE	53
	5.6 SYSTEM DESIGN CONSIDERATIONS	54
	5.7 ALTERNATIVES IN ASSESSMENT	55
	5.8 UNCERTAINTY PERSPECTIVE	55
6	REFERENCES	71
<u>Appendix</u>		
A	ABBREVIATIONS	73

LIST OF FIGURES

<u>Figure</u>		<u>Page</u>
2.1	Nevada Model Area for MPS Deployment.	16
2.2	Hexagonal Pattern of Launch Points.	17
2.3	Launch Point Modeling Module.	18
2.4	Attack Pattern, 1 Megaton Attack.	19
2.5	Attack Pattern, 3 Megaton Attack.	19
3.1	Concept of an Equivalent Dose Rate Configuration. . . .	33
3.2	Fallout Field Definitions	34
3.3	Dose Rate Computation at DELFIC Grid Points	34
3.4	Dose Rate Contributions at Pseudo Monitor Points. . . .	35
3.5	Particle Count as a Function of Size Classes and Wafers.	35
3.6	DELFC Field Definition From a Single Cloud Level	36
3.7	Downwind Transverse Dose Rate Distributions - 1 MT. . . .	37
3.8	WMO Weather Stations Near Nevada MX Site.	40
4.1	LAMB Tracer Particle Positions.	43
4.2	Comparison of Multiburst Shock Effects for Several Double Burst Separations.	45
4.3	Direction of Velocity Vector of Fireball Center Immediately After Shock Arrival, As a Function of Burst Separation, For Two Simultaneous 1 MT Bursts. . . .	47
4.4	Torus Time For Different Burst Separations.	48
4.5	Fireball Growth (Single Burst Versus Multiple Burst)	49
5.1	H+1 Hour Dose Rate Distribution, Moderate Wind Case	57
5.2	H+1 Hour Dose Rate Distribution, High Wind Case	58
5.3	Dose Rate Distribution, First Quarter	59

LIST OF FIGURES (Continued)

<u>Figure</u>		<u>Page</u>
5.4	Dose Rate Distribution, Second Quarter.	60
5.5	Dose Rate Distribution, Third Quarter	61
5.6	Dose Rate Distribution, Fourth Quarter.	62
5.7	Annual Envelope of Dose Rate Distribution, Forty Wind Samples.	63
5.8	Parametric Assessment of Fallout Hazard, 100 Rads Allowable Dose.	65
5.9	Dose Rate Time History, Monitor Point A	66
5.10	Dose Rate Time History, Monitor Point B	67
5.11	Dose Rate Time History, Monitor Point C	68
5.12	Dose Rate Time History, Monitor Point D	69
5.13	Dose Rate Time History, Monitor Point E	70
Table 5.1	Dose Rate Distribution Summary	64

SECTION 1

INTRODUCTION

1.1 PROBLEM

The analysis reported here is concerned with the residual activity due to fallout which might be experienced on an MX site following a massive attack. There are two principal interests:

- a) the hazard posed to post-attack maintenance crews which could preclude their early entry into the site
- b) the potential vulnerability of the MX system (missile and ground-based equipment) electronics to fallout activity during breakout, erection and launch.

1.1.1 Bounding the Problem

A simple estimate can be made of the average activity by assuming that all of the fallout is deposited uniformly on the site. The activity expressed in terms of the dose rate, \dot{D} , at one hour after the burst, is then

$$\dot{D} = N \cdot W \cdot FF \cdot K / A$$

where N is the number of bursts, W is the yield, FF is the fission fraction, A is the site area. The other term, K , is a normalization in units of R/Hr per kt of fission yield over a unit area. Typically this K -factor⁽¹⁾ is 2900 R/Hr kt⁻¹ mi². Considering an illustrative example where there are 5000 weapons of 1 Mt yield and 50 percent fission fraction and the site area is 5000 sq. mi., the resulting dose rate is about 1.5×10^6 R/Hr at 1 Hr. This simple calculation, however, is an extreme over-estimate because it assumes all of the activity is deposited on-site whereas the actual on-site fraction is going to depend on local wind conditions (Only in essentially a zero-wind situation could such an estimate be considered realistic).

1.1.2 Refinements

The next level of complexity of such a calculation requires an explicit treatment of advection in local winds and grounding of radioactive particles using available fallout models. This is the approach followed for the results presented here. The fallout model employed is the DELFIC⁽²⁾ code and is the most accurate available. Rather than use "mean" winds or "most probable" winds, actual wind data, randomly selected from that recorded at reporting stations in the vicinity of the MX site, are used. The methodology is presented in Section 3. This leads to dose rates associated with a probability of occurrence as will be discussed in Section 5.

1.2 OFFENSIVE THREAT

The specific scenario for the analysis was chosen by the MX-SPO. The laydown involved 3538 surface bursts of 1 Mt yield on the Nevada model site. The spacing between bursts was 7000 ft. Details of the laydown are given in Section 2.

1.3 ASSUMPTIONS

Because of the spacing between bursts and the assumption of near simultaneous detonations, it is reasonable to expect that there would be interactive effects between bursts. As discussed in Section 4, however, there is no adequate model at present, for estimating the effect of the interactions on fallout. Hence, the calculations here assume superposition of the fallout patterns from individual bursts.

1.4 FINDINGS

The results of this work are summarized as follows: the fallout radiation hazard to MX resulting from the hypothetical attack of 3538 1 Mt surface burst weapons at the Nevada site must be regarded as a severe one. Median dose rates at H+1 are estimated to be in the 50,000 R/Hr range with variations of plus and minus a factor of 2 for

the 40 wind samples that were evaluated. However, the determination as to whether MPS deployments under consideration are feasible is dependent on a number of additional factors. If vertical shelters of the silo type are being contemplated for example, the shielding associated with that kind of construction could conceivably prove effective depending on such factors as dose criteria, overall system functional design and launch delay periods. Transmission factors (the ratio of inside dose to outside dose) for closed shelters with 3 feet of earth cover are typically in the 0.005 range and silo factors could be comparable. Crews need not be located at the launch points themselves of course, and despite the fact that allowable doses for electronic equipment are expected to be several orders of magnitude greater than those for personnel, one cannot discount the possibility that the vulnerability of equipment might be the limiting constraint. High local dose rates and significant launch delays following an attack could cause such a situation to obtain.

1.4.1 Illustrative Problems

Two conditions of obvious relevance are suggested by the foregoing discussion: first, the radiation hazard to equipment, assuming there will be some period of delay before launch; and second, the vulnerability of missile maintenance crews that might be needed to perform repairs on missiles rendered temporarily ineffective by the initial effects of the attack. In the latter case, it would be absolutely essential to minimize exposure time, as will be shown below. However, before presenting illustrative calculations, it is appropriate to note that whole body radiation doses in the 100-200 rad range, although not expected to produce deaths in humans, do normally induce nausea and vomiting within 3-6 hours of exposure --- a highly undesirable condition from both the standpoint of effectiveness and morale. One should keep these factors in mind when considering the following calculations, which are presented to illustrate the dependence of operational feasibility upon system design and tactical factors, especially time.

• CASE I

GIVEN: Missile maintenance/repair crews must be inserted into contaminated areas to effect repairs following a nuclear attack. The missile must be raised out of the silo to do the necessary work. The required stay time is 1 hour and the allowable dose is 100 rad.

DETERMINE: The earliest entry times for H+1 dose rates of 50,000 R/Hr and 100,000 R/Hr.

ANSWER: Approximately 7 and 13 days after the attack for 50,000 R/Hr and 100,000 R/Hr at H+1 respectively.

• CASE II

GIVEN: The fallout associated with the attacks of CASE I arrives at H+1 hour. MX missiles are emplaced in covered silos with a transmission factor of .005. Allowable dose for electronic equipment is 100,000 rad.

DETERMINE: The total doses accruing to missiles within the silos at 7 days if the DR_1 is 50,000 R/Hr and 13 days if the DR_1 is 100,000 R/Hr.

ANSWER: Approximately 300 and 1700 rad respectively.

• CASE III

GIVEN: Missile repair crews must be inserted into contaminated areas to effect repairs following a nuclear attack. Repairs can be accomplished inside the closed silo. Insertion and extraction of crews can be accomplished by helicopter in one minute, during which time crews have no protection. Transmission factor for the silos is 0.005. Allowable dose to personnel is 100 rad, and required stay time is 1 hour.

DETERMINE: Earliest insertion times for repair crews for H+1 dose rates of 50,000 and 100,000 R/Hr.

ANSWER: Approximately H+12 hours for $DR_1 = 50,000$ R/Hr and H+21 hours for $DR_1 = 100,000$ R/Hr.

1.4.2 Implications

The operational implications of these examples are fairly obvious. To enable additional estimates of this type using other values for entry times, stay times, transmission factors and dose rates, a parametric chart is provided in Section 5, Figure 5.8. Obviously the same can be done for electronic equipment if it appears to be a candidate for the limiting constraint role. As a matter of interest, the time histories of dose rates at several monitor points selected from the proposed deployment area also are given in Section 5, Figures 5.9 through 5.13. In each instance, peak dose rates were achieved prior to H+1, usually at or near H+30 minutes. The implications of the fallout radiation hazard for operational impact are numerous and in the final analysis they could be crucial. While it is very useful to estimate the severity of the fallout hazard prior to attack, it is nevertheless clear that a post-attack assessment will be required. It is highly desirable that there be a capability to determine rapidly (certainly within a few hours, hopefully sooner) which of the occupied launch points have survived the initial nuclear effects of the attack and what the actual radiation dose rates are at those surviving sites. This suggests that status sensors should be emplaced to reflect radiation levels as well as mechanical readiness at the launch sites. Clearly, it is preferable to be able to perform maintenance and repairs to missiles inside the shelters so that radiation exposure levels are minimized. Command, control, communications and logistics also will play a major role in determining the post-attack effectiveness of any MX MPS deployment, but it is not the purpose of this report to examine these considerations. Nevertheless, it must be recognized that any assessment of the fallout radiation hazard is necessarily dependent on the degree to which these operational capabilities exist, and it is for this reason that they are mentioned.

1.4.3 Summation

Despite the severity of the anticipated fallout hazard to MX MPS deployment under consideration, it would be premature at this point to conclude that fallout in itself would render such deployments infeasible. A sound decision on that question can be reached only after alternative designs of the system have been analyzed and compared, including consideration of initial nuclear effects. We believe the parametric presentation of the key fallout-related factors as contained in this report provides a reasonable measure of the residual radiation hazard and hence a rational basis for remaining analytical work. A highly compressed version of our findings to date is as follows:

- The fallout hazard to MX must be regarded as severe -- median dose rates at H-1 are estimated to be in the range of 50,000 R/HR plus and minus a factor of two due to wind variation
- Vulnerabilities of [both] equipment to both prompt and residual nuclear effects must be considered in achieving a balanced system design. Depending on the final operational and maintenance procedures adopted, personnel vulnerabilities may also be a factor requiring further analyses.
- At this point, a parametric approach appears appropriate in assessing the magnitude of the fallout hazard.
- System feasibility is highly dependent on a number of factors in addition to cost. Some of these are:
 - functional design
 - operational tactics and policies
 - repair scenarios
 - correlation of fallout hazard with expected prompt effects on the system

3

It has not been possible to perform a comprehensive uncertainty analysis of the calculated dose rates. The above median value is a best estimate that could be affected by several factors. The first of these must be the potentially significant effect of interacting adjacent bursts on cloud height. If the clouds from such bursts stabilize at a higher altitude than would be expected in the single burst case, less of the fallout would occur on-site. Typical of other factors that might affect the calculations is the size distribution of the entrained soil.

SECTION 2

SITE MODELING AND SCENARIO PARAMETERS

2.1 THE DEPLOYMENT AREA

The Nevada site is one of three currently under consideration for possible multiple protective structure (MPS) deployment of MX. The remaining two sites are located in the White Sands, New Mexico area. The Space and Missile Systems Organization (SAMSO), Air Force Systems Command located at Norton AFB, California currently considers that the Nevada site appears to offer the best combination of range capability, weather and topographical conditions and it was therefore assigned first priority in terms of assessment of the fallout hazard. The Nevada site contains more than 50 irregularly-shaped land parcels which potentially are suitable for MPS deployment of MX. These land parcels lie within a rectangular area bounded by west longitudes 114° and 118° on the east and west and by north latitudes $37^{\circ} 15'$ and $39^{\circ} 15'$ on the south and north (Figure 2.1). These boundaries enclose an area of nearly 30,000 square statute miles, only about one-quarter of which (7540 square statute miles) is contained within the parcels themselves.

2.2 THE CONCEPT

The basing concept is one designed to create an unfavorable "exchange ratio" for the attacker, i.e., with thousands of aim points (not all of which would be occupied by a missile at a given time), the ratio of attacking missiles required to insure destruction of a significant portion of the MPS-deployed ICBM force is disproportionately high; perhaps 4 to 1 or 5 to 1. It is assumed of course, that the attacker does not know which sites are occupied. The need for this kind of disproportionate exchange ratio is brought about by the greater number of Soviet ICBM's allowed under the SALT I treaty and their superior throw-weight capability which allows fractionation of

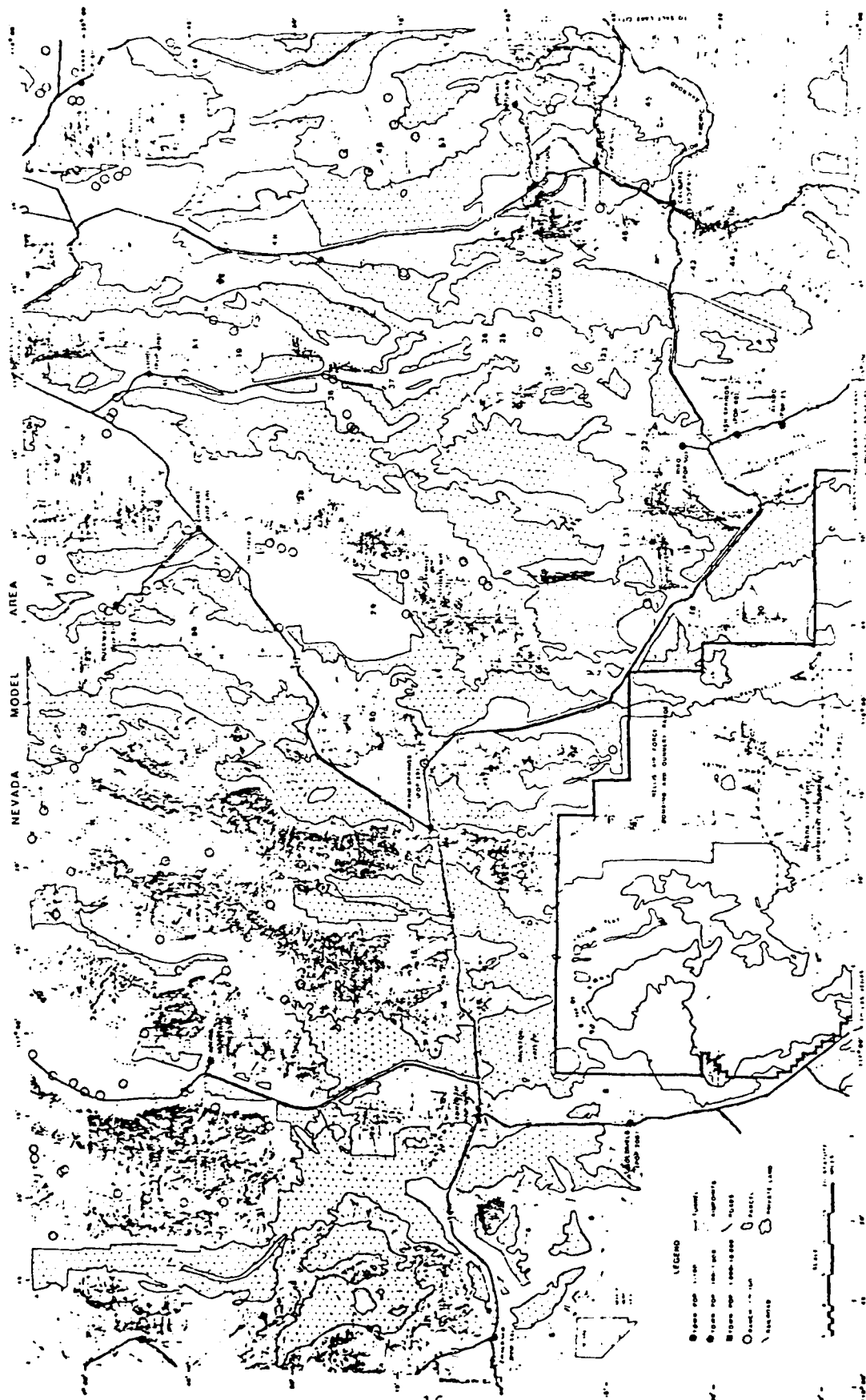


Figure 2.1 Nevada Model Area for MAP Deployment

their payload and hence large numbers of reentry vehicles. The MAP concept is intended to deny the Soviets any decisive advantage in a first strike and thus enhance nuclear deterrence.

2.3 MODELING DEPLOYMENT CONFIGURATION

The deployment pattern selected by SAMSO appears as a "honey-comb" of regular hexagons with the launch points located at the vertices and centroids of the hexagons (Figure 2.2). The pattern spacing of initial interest was one in which the sides of the hexagons were

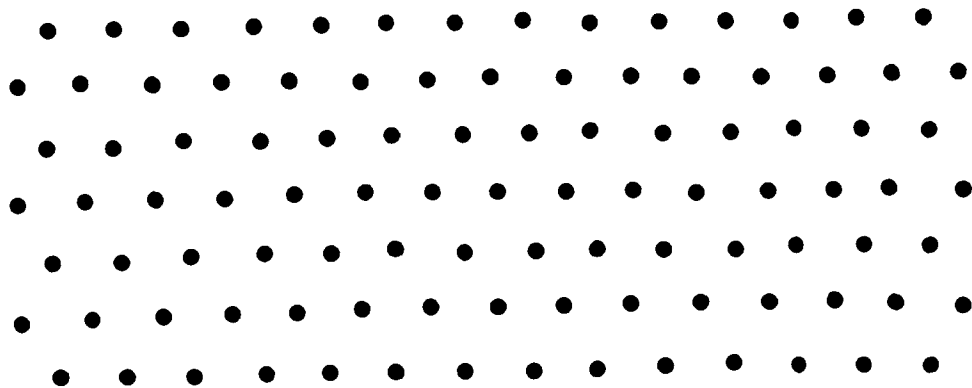


Figure 2.2 Hexagonal Pattern of Launch Points

7000 feet long, although other spacings are also to be examined. To obviate the need to hand-plot individual launch points, a "module" of the hexagonal pattern was developed (Figure 2.3) and manually fitted to the unique shapes of the land parcels. The module was chosen in a manner which caused contiguous modules to propagate an unbroken pattern of regular hexagons at the desired spacing. Where appropriate, segments of the module were used to accommodate the unique shapes of the land parcels while maintaining continuity of pattern. Radiation monitor points were located in each of the modules so that the DELFIC Model radiation dose rates could be associated with each module throughout the proposed deployment area. These dose rates formed the basis by which to measure the extent of the fallout hazard.

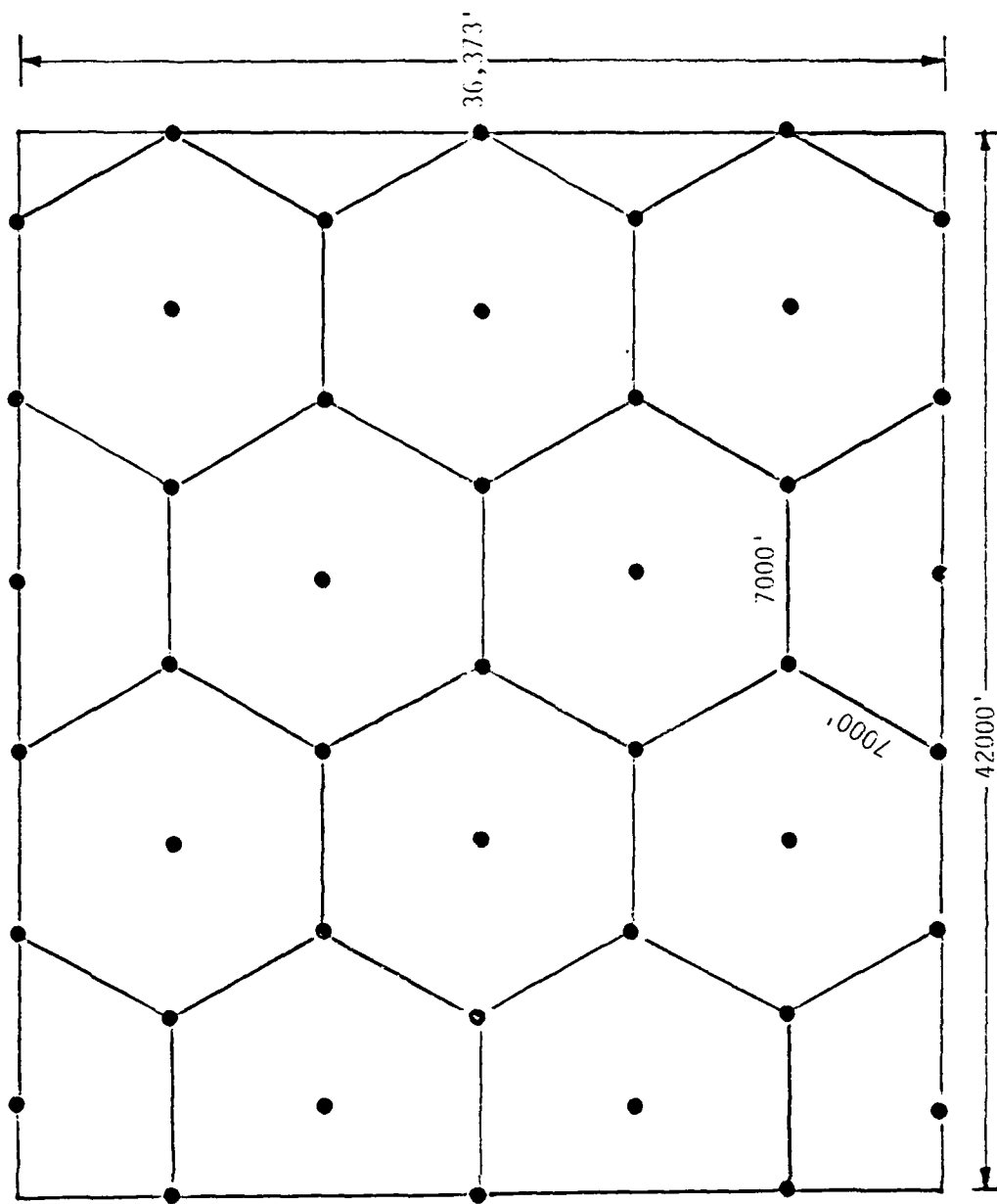


Figure 2.3 Launch Point Modeling Module

2.4 ATTACK SCENARIOS

The two attack scenarios provided by SAMSO were simple and straightforward. In the first one, a one megaton weapon is detonated at each of the launch points located at the vertices of the hexagons comprising the "honeycomb" pattern (Figure 2.4). Launch points located

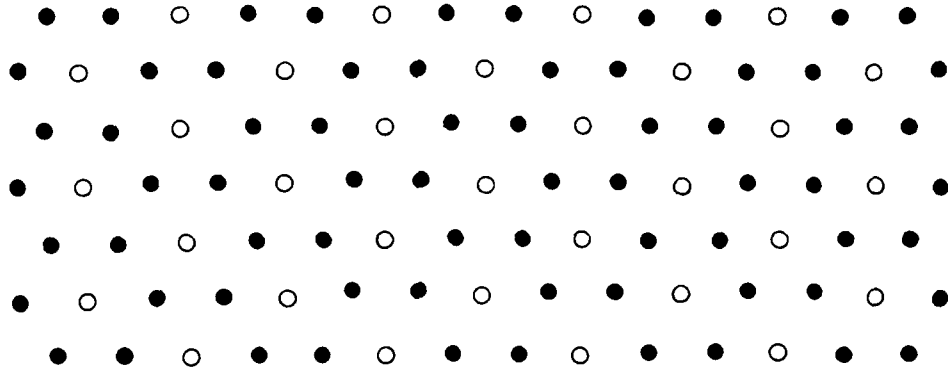


Figure 2.4 Attack Pattern, 1 Megaton Attack. Darkened launch points receive surface-burst weapons.

at the hexagon centroids did not receive a weapon. The second scenario involved three megaton detonations at every other vertex of the pattern (Figure (2.5)). Simultaneous detonations were assumed in both cases,

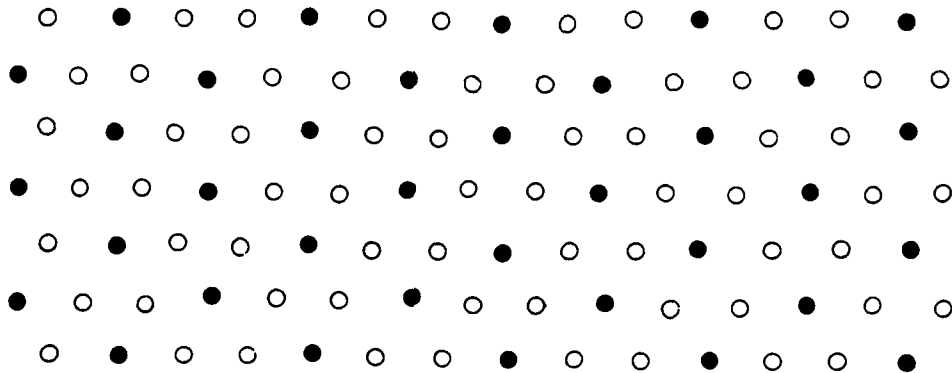


Figure 2.5 Attack Pattern, 3 Megaton Attack. Darkened launch points receive surface-burst weapons.

e.g., the "spike" attack tactic. The fission fraction values for the two yields were provided by SAMSO so as to be consistent with intelligence estimates. The effects of weapon system reliability (e.g., probability of arrival) were deliberately ignored as was accuracy so that a reasonable upper bound measure of the fallout hazard could be obtained. In effect then, all targeted weapons arrived simultaneously and precisely at the intended aim point. The result of this, of course, is a somewhat overstated estimate of the radiation hazard, but for the purpose of determining design specifications and in light of the many uncertainties attendant to such an attack (e.g., attack intensity, fission fraction, cloud height, particle size distribution), the assumptions of the scenarios appear to be appropriate. This report addresses only the results of the first scenario, i.e., the one-megaton weapon attack. Similar attacks involving three-megaton weapons would scale roughly in proportion to the yield.

SECTION 3
METHODOLOGY

3.1 CONCEPTS

3.1.1 Approach to the Multi-Burst Problem

This section describes the concepts and procedures used to compute the fallout hazard for the MX site due to a postulated attack. The methodology employs the DELFIC code, Ref. 2, for the computation of cloud rise, activity, and transport. A formulation is developed which permits fallout data from a single burst DELFIC run to be utilized for the computation of the multi-burst environment using linear superpositioning. The utilization of linear superposition invokes constraints on weapon time of arrival, wind variation, and burst interaction. The following assumptions were appropriate: all bursts are of equal yield and detonated simultaneously; the variation of wind speed and direction are functions of altitude only (time and spatially invariant wind fields); and burst interaction effects are neglected.

3.1.2 Treatment of Assumptions

Regarding these three assumptions, the first one is part of the attack scenario specified by SAMSO. The time and spatially invariant wind fields have no adverse impact on the analysis for the MX site for the following reasons: the extent of land area is small for the purpose of wind field definition; the number of wind stations with complete data is inadequate and they are too widely spaced to define a "better" wind field than the single station close by; the majority of fallout lands on site during the first few hours; and most important, the variations due to wind time dependence would result in field depositions that would be between the minimum and maximum depositions of the strongest and weakest wind fields and thus provide little additional information of value. With regard to possible burst interactions, current state-of-the-

art thinking addresses two phenomena: the change in stabilized cloud height and lateral cloud motion due to assymetrical bursts. For a given wind field as considered here, the amount of fallout matter landing on the site is proportional to the stabilized particle altitude. Thus if multiburst interactions alter the stabilized cloud height, the variations in on-site fallout will vary in nearly direct proportion to the variations in altitude induced by the interactive effects. A higher stabilized cloud would give less on-site fallout and a lower stabilized cloud height would yield more. It will be shown in Section 5 that for the Nevada site and the 40 winds investigated, wind variations can alter the average on-site dose rate by a factor of 3. The variation in predicted cloud height due to multiburst effects is believed to be fractional. However, it is possible that significant interactions may take place in the interior region of the attacked area, and these effects are ignored in this study. Based on these considerations, the basic assumptions should not significantly impair the validity of the answers generated by the utilization of superposition.

3.1.3 Program Development

Linear superposition implies that the activity at any point in the fallout field is the sum of the activity at that point from all the weapons. Thus we detonate a specified number of weapons and add their contributions at each point of interest. This could present a problem with regard to computer time since several thousand weapons are to be considered. In light of the assumptions outlined above, we can compute the fallout hazard at an arbitrary number of m monitor points due to a weapon laydown consisting of n arbitrarily located bursts by computing the fallout field of a single weapon. In order to do this we employ the concept of an equivalent dose rate configuration. This concept is described below.

3.1.4 Equivalent Dose Rate Configurations

By linear superposition, the dose rate at any point from n detonations is equal to the sum of activity at that point contributed by all the weapons. Under the stipulations above, this is exactly equal to the fallout from one weapon summed over $n-1$ pseudo monitor points plus the actual monitor point. A pseudo monitor point is a location in the fallout field of a single weapon that has the same geographical location relative to that burst point as the actual monitor point has to one of the bursts of a multiburst laydown. The configuration of pseudo monitor points is the dose rate equivalent configuration. This concept is illustrated in Figure 3.1. Figure 3.1a shows the dose rate at a designated monitor point MP_i , being affected by a contribution of fallout from each of four bursts, BP_j . The dose rate at MP_i is given by

$$D_{MP_i} = \sum_j D_{BP_j} \quad j = 1, 4$$

Under the specified assumptions, the identical value D_{MP_i} can be computed using the dose rate equivalent configuration shown in Figure 3.1b. In this figure, one burst point location was selected at random. A number of pseudo monitor points were generated equal to the number of burst points. The pseudo burst points are defined by the position vectors \bar{S}_j , which are identical to the original position vectors \bar{R}_j except for their point of origin. Whereas in Figure 3.1a, the vectors originated at each burst point and located the monitor point of interest, in Figure 3.1b, the vectors \bar{S}_j originate at one of the burst points BP_2 , and define four pseudo monitor points. One of these pseudo points is the actual point of interest. Each pseudo monitor point PMP_j , of Figure 3.1b occupies the identical position in the fallout field of the single burst, as the single monitor points occupies in the field of each of the four burst in Figure 3.1a. Thus the sum of fallout at each of the pseudo monitor points is equal to the sum obtained from Figure 3.1a. We have then

$$D_{MP_i} = \sum_j D_{PMP_j} \quad j = 1, 4$$

From this we see that each actual monitor point requires a set of pseudo monitor points equal to the number of burst points to perform the superpositioning. Thus if we have m monitor points and n burst points we will require m x n pseudo monitor points located about a single burst point in order to compute the total dose rate at each monitor point due to the multiburst laydown.

3.1.5 Mathematical Formulation

With reference to Figure 3.1 the equation defining the pseudo monitor points for the general case of m monitor points and n burst points are easily determined. Let $(MPX, MPY)_i$ be the x and y locations of the m monitor points and $(BPX, BPY)_j$ be the x and y locations of the n burst points. The matrix of m x n pseudo at monitor points then becomes

$$PMPX_{i,j} = MPX_i + (BPX_k - BPX_j)$$

$$PMPY_{i,j} = MPY_i + (BPY_k - BPY_j)$$

where $i = 1, m$; $j = 1, n$ and k is one burst point selected as a reference. Reference burst k is selected from the burst point set n and is constant. The total fallout activity at any monitor point i is then

$$D_{MP_i} = \sum_{j=1}^n D_{PMP_j}$$

where D_{PMP_j} is the activity at location $(PMPX, PMPY)_j$ in the field of the reference burst k.

3.1.6 Field Definition

The methodology described above is conceptually one of taking a single burst and moving it around to each burst point and adding the fallout contributions at each affected monitor point. Because of these translations, the defined field of the single weapon must be large enough so that regardless of where it is positioned in the actual fallout

field, there will be no undefined areas, i.e., undefined in terms of computer recognition in the calculation. In Figure 3.2, a burst is located at the center of the actual fallout field with length L and width W. In order to permit total coverage of the actual field area by the fallout field of the single weapon, that weapon's fallout field must be defined in a area whose length and width are 2L and 2W respectively. This is true for a burst at the center and an arbitrary fallout field. Since the location of the reference point is arbitrary, we can say that field of definition for the single burst is an area with dimension (2L x 2W) centered about the burst point. The significance of this definition is that in order to use the equivalent dose rate configuration concept, there must be a means of quickly and accurately defining fallout quantities at any point in the single weapon field when that single weapon field has four times the area of the actual field.

3.1.7 Modifications to DELFIC

The DELFIC program, Reference 2, provides for the definition of a fallout field by means of a dose rate map. This map consists of dose rate values on a rectangular grid network. The size of the grids is a user-determined option. The most obvious approach for the utilization of DELFIC is to use directly this output map to find the required dose rates. This would necessitate interpolation of dose rate since the pseudo monitor point locations in general would not be the same as the map grid points at which the dose rates are defined. The size of the MX field in Nevada is approximately 223 x 354 kilometers. For an arbitrary wind, the single weapon fallout field would have to be defined for an area of 446 x 708 kilometers. If one kilometer resolution were desired, approximately 3.1×10^5 storage allocations would be required to store the map. A 10 kilometer resolution would require approximately 3100 storage locations. The problems that must be addressed for direct map utilization are then grid resolution and interpolation. The major drawback of this approach however is not so much in the computer implementation but the fact that it is impractical to establish dose rate time dependencies via this method. This stems from the fact that it

could only be done by making a separate map for each time increment comprising the time interval over which the distribution is desired. For this reason, and also to avoid criticism of fallout models that may interpolate artificially, it was *decided not to employ this approach*. Instead, the principles employed in the DELFIC map generating subroutines were used to compute the dose rates at a point directly, without the need for a map and the attendant interpolations.

3.1.8 Computation of Fallout at a Point

The principle used to generate the dose rates for the DELFIC map is illustrated in Figure 3.3. For horizontally non-subdivided cloud layers, each particle size class is represented by a central location (landing point) surrounded by a square whose area is equal to the circular cloud area from which it came (plus an accounting for diffusion, if appropriate). With the wafer on the ground, the uniform dose rate of that wafer is added to each grid point that it covers. This process is repeated for each wafer that lands in the map region. These computations are performed in the output processor, *module 5, of the DELFIC program*. They are carried out using data contained by the particle transport file generated by the transport module 4. The procedure by which the dose rates were computed for this effort is illustrated in Figure 3.4. Since we are only interested in the dose rates at the pseudo monitor points, only those wafers falling within the area of possible influence about the point of interest are considered. The area of possible influence is a square, centered about the pseudo monitor point, whose area, is equal to the maximum horizontal cross sectional area of the cloud. No diffusion was used in this study. Since all wafers must be less than or equal to this area, only those whose landing points that are within the square could contribute to the dose at the center. Further, their size and/or location must be such that they overlap the central point. Thus, in Figure 3.4, wafer 1, even though inside the area of possible influence will not contribute. Neither will wafer 2 because it is outside the area. Wafers such as number 3

will contribute to the dose rate at (PMPX, PMPY). The amount of contribution is equal to the uniform area activity of that wafer. To provide some computational efficiency, the DELFIC module 4 transport file is compressed, by deleting all landing points outside the single burst fallout field of interest. The particles remaining are then sorted by x-coordinate. This permits rapid identification during one computational sequence, of all particles in the region of possible influence about a point. The DELFIC map grid point dose rate computation and the method of computing dose rates at a pseudo monitor point are entirely equivalent with regard to the dose value that will be computed provided that the grid point and pseudo monitor point are identical.

3.1.9 Comments on the Methodology

The direct computation of fallout dose from particle landing points is technically superior to map interpolation. It has one possible drawback -- computer execution time is sensitive to the number of particles landing in a region of possible influence, and other things remaining constant, is directly related to the total number of particles in the cloud. The determination of selecting a number of particles to provide adequate field definition while limiting required computer execution time is discussed in the paragraph on input specifications.

3.1.10 Determination of Dose Rate Time Dependency

The determination of the dose and dose rate time dependency was done as follows: the actual time of arrival of each particle is available on the transport file. Each weapon fallout field was defined by approximately 1000 wafers. For the case under consideration, with 3538 burst points, potentially many thousands of wafers could, and do, effect a designated monitor point. Instead of tracking each wafer, small time intervals were established, typically 0.01 hours. All arriving wafers corresponding to an interval were grouped in that interval. From these time-sorted wafers, the following three distributions were computed.

Time dependency of the Normalized One Hour Dose Rate - D.R. H+1 (t_k) this quantity, from time 0 to any time t_k was computed by

$$D.R. H+1 (t_k) = \sum_{j=1}^k DR (H+1)_j$$

where $DR (H+1)_j$ is the accumulated one hour dose rate in time interval j .

Time Dependent Actual Dose Rate - $DR (t_k)$

The actual dose rate at time t_k was computed using the $t^{-1.2}$ relationship as follows:

$$DR (t_k) = t_k^{-1.2} \sum_{j=1}^k DR (H+1)_j$$

Total Accumulated Dose - D

The total accumulated dose from time 0 to time t_k was computed as follows.

$$D (0, t_k) = 1/2 \sum_{i=1}^{k-1} (t_{i+1} - t_i) (t_{i+1}^{-1.2} + t_i^{-1.2}) \sum_{j=1}^i DR (H+1)_j$$

3.1.11 Determination of Percent Activity On Site

The computation of percent activity landing on site was as follows: the fallout field was placed at each burst point and all of the wafers landing within the actual field were identified. The normalized one hour dose rate contribution of each wafer was multiplied by the respective wafer area and summed over the entire field. The computation of total lofted mass on site was also done, since it involved no additional effort. The results of these computations appear in Section 5.

3.1.12 DELFIC Input Parameters

The version of DELFIC used for these computations was obtained from United States Army Ballistic Research Laboratory (USABRL) and is known as the Mark V version. Some of the more significant parameters selected are listed below with the values used.

Yield	1000 Kiloton
Atmosphere	30° North, July
Soil	Silicious
Ground Roughness Factor	0.7
HOB	0
Solidification Temp	1673 °K
Time Limit	10 days
Ground Zero Height	1500 Meters
Topography Height	1500 Meters
Neutrons per Fission	1.4
Fission Type	P239HE
Wind	See Below
Number of Levels	See Below
Number of Size Classes	See Below
Size Class Mean	0.407 Microns
Standard Deviation	4.0

3.1.13 DELFIC Fallout Field Computation

3.1.13.1 Parametric Determination of Number of Size Classes and Cloud Levels

As indicated previously, the computer execution time for the precise formulation (i.e., precise with regard to computing exactly what DELFIC would compute based on its methodology) is dependent on the number of particles. A sensitivity analysis was done to determine the tradeoff of accuracy vs. computer running time requirements. It was therefore necessary to determine the most cost-effective number of particles to use while retaining acceptable accuracy. A series of DELFIC runs were made using a 10.3 m/sec wind. Each run had a different number of size classes and cloud levels. A designation of $m \times n$ was adopted. The first number is the number of size classes. The second is the number of cloud levels. Six different combinations were examined. These were 10 x 10, 20 x 20, 30 x 30, 50 x 50, 70 x 70 and 100 x 100. The actual number of particles corresponding to each of these runs is nearly equal to the product of m and n . The variation in particle count is shown in Figure 5 and is referenced to the parabolic curve $y = x^2$.

3.1.13.2 Generation of the Fallout Field

Before looking at the results of this analysis, it will be instructive to look at Figure 3.6. This figure depicts the manner in which DELFIC generates a fallout field. A number of square wafers comprising the size classes are dropped from a cloud and transported by the wind. Close in, the wafers overlap and a continuous and reasonably smooth variation in fallout can be obtained. Sooner or later, depending on number of sizes and distance from ground zero, the situation depicted for the far field will occur. That this is inevitable can be deduced from the fact that there is an upper limit of 200, on the number of size classes. Thus even with 200 wafers, and all wafers edge to edge, the farthest that we could get down wind is $200\sqrt{\pi} R_c$ beyond the point of initial fallout before "holes" would develop. (The squares have the same area as the round disks with cloud radius R_c , thus the term $\sqrt{\pi}$). For an actual case, there would be some filling of holes by particles from other layers. Fortunately, the dose rates for far fields where gaps can occur are usually low. This problem should however be considered when larger areas are to be investigated. The proposed MX field in Nevada is over 300 km wide. For this distance, a 1 Mt cloud layer with 100 size classes could not go from end to end without gaps. As was mentioned, the gaps are not of great significance in themselves, so long as they are covered by wafers from some other layer. Thus the validity of a down field fallout prediction can be judged by the change in transverse distribution (i.e., normal to the "hotline") as a function of particle count. A satisfactory limit on transverse distribution at the desired downwind distance would indicate the particle count that would be acceptable.

3.1.13.3 Determination of Particle Count

The results of the analysis outlined in paragraph 3.1.13.1 are presented in this paragraph.

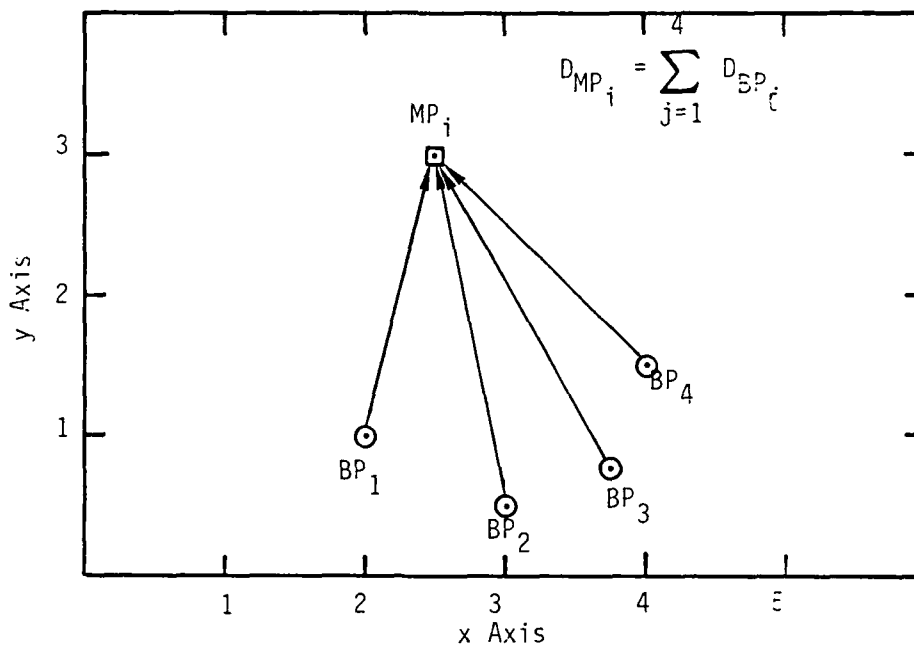
The downwind transverse distribution of normalized dose rate for a 1 MT burst is shown in Figure 3.7, for downwind distances of 10,

60, 150, 250, and 350 kilometers. At 10 km, Figure 3.7a, adequate agreement can be said to exist for the five m x n combinations shown. At 60 km, the 10 x 10 shows a significantly different trend. At 350 km, there is no fallout from a 10 x 10. The larger three cases -- 50 x 50, 70 x 70 and 100 x 100 are very similar over the entire downwind range. A 50 x 50 matrix would be too time consuming because of the wind effects study intended. It was decided to use the 30 x 30 which gave very good agreement with the 3 larger sizes up to 250 km. It would have taken approximately 2½ times as long to do a wind sensitivity study using the 2696 particles of the 50 x 50 as opposed to the 1042 particles of the 30 x 30 set. Based on the findings of Figure 3.7d this increase appeared unwarranted.

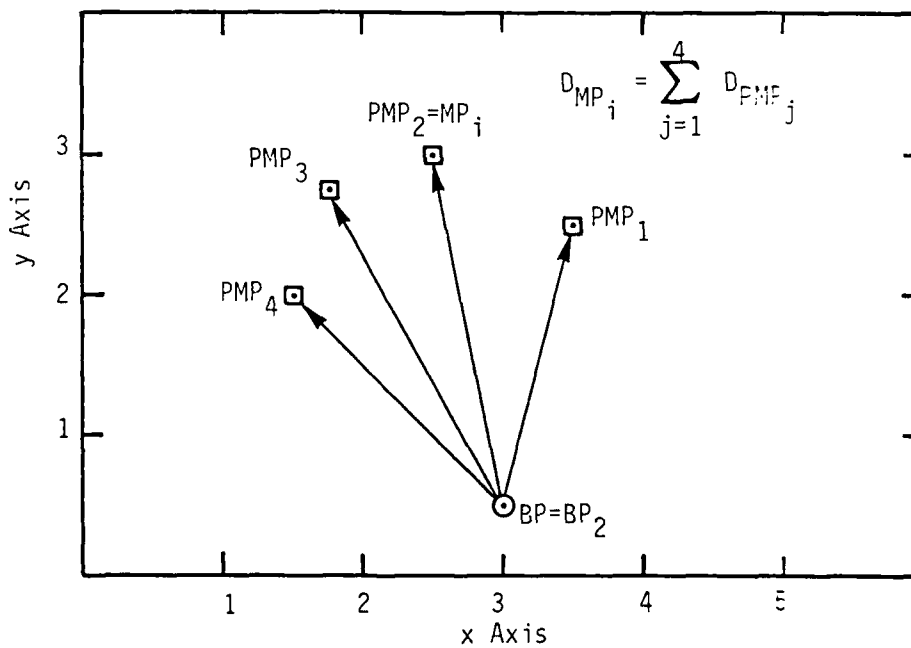
3.1.14 Wind Profile Data

The objective of this effort was to predict MX site fallout hazards. Actual wind profiles were used. To this end, rawinsonde data in TDF 56 VAR format for the years 1971-1985 were used to establish the wind data base. This information is obtainable from National Oceanic and Atmospheric Administration, Asheville, N.C.. Based on WMO station data listed in Reference 3, wind station locations in the vicinity of the proposed Nevada and Arizona site were obtained. These are shown in Figure 3.8. Of all the stations in the vicinity of the Nevada site, only data from two stations were available. These are the two numbered stations in Figure 3.8, station 72486 and station 72583. Because of its proximity, station 72486 was used to obtain wind profiles for most of the year. 1975 was arbitrarily chosen to be the reference year. Approximately three months of consecutive data was missing from station 72486. For the missing months, data was taken from station 72583. Wind data was not available for every day of the year. Of the data that was available, some of it was inadequate for our purpose. As a result, approximately 340 readings from station 72486 and 470 readings from station 72583 were found suitable for consideration as wind profiles.

Ten days from each yearly quarter were selected, the 10 days being spread over the period as evenly as possible. The criteria for a profile to be considered were that it contained at least 6 altitude entries below 20,000 meters, that the first reading be below 2000 meters and that all entries be present, i.e., altitude, velocity, and direction defined.



(a) Dose Rate at MP_i Due to Four Bursts



(b) Dose Rate Equivalent Configuration of (a)

Figure 3.1 Concept of an Equivalent Dose Rate Configuration

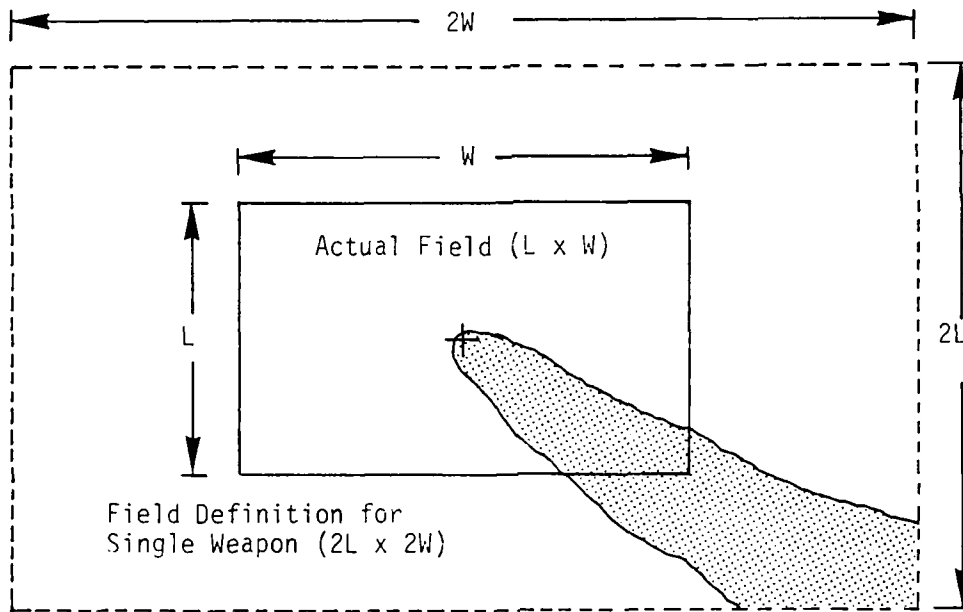


Figure 3.2 Fallout Field Definitions

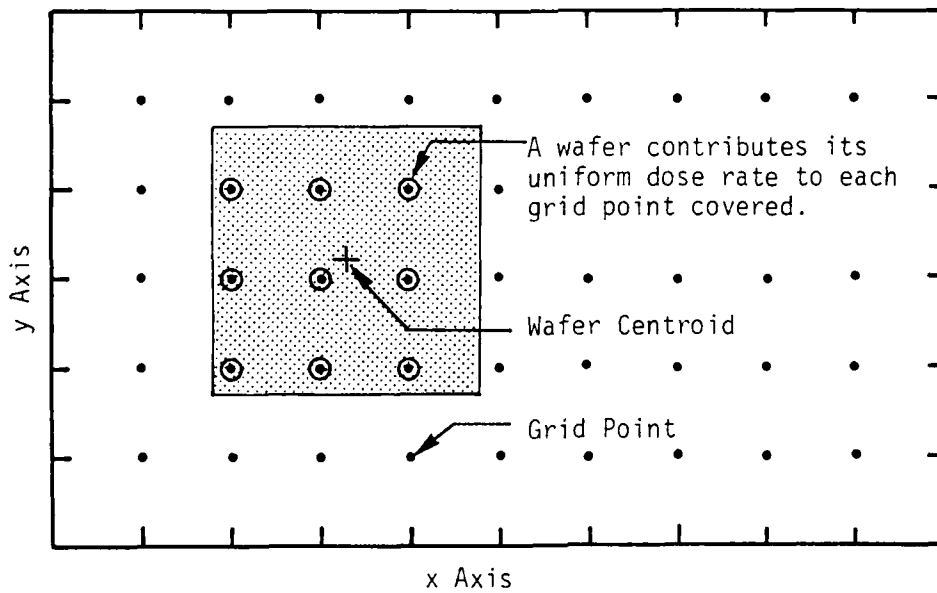


Figure 3.3 Dose Rate Computation at DELFIC Grid Points

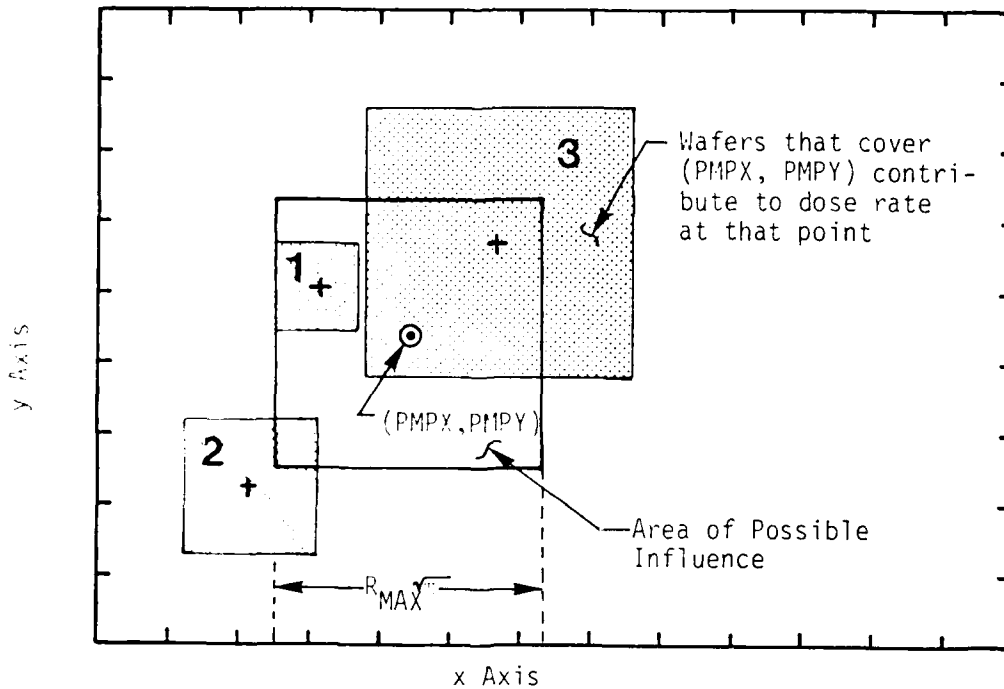


Figure 3.4 Dose Rate Contribution at Pseudo Monitor Points

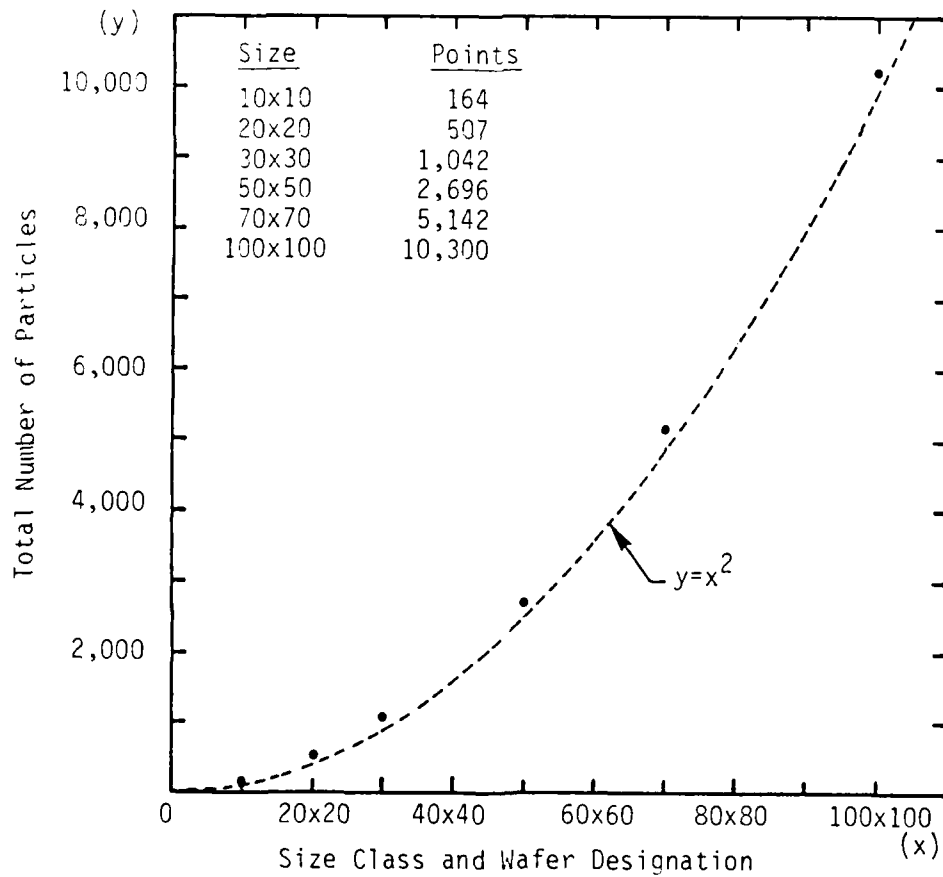
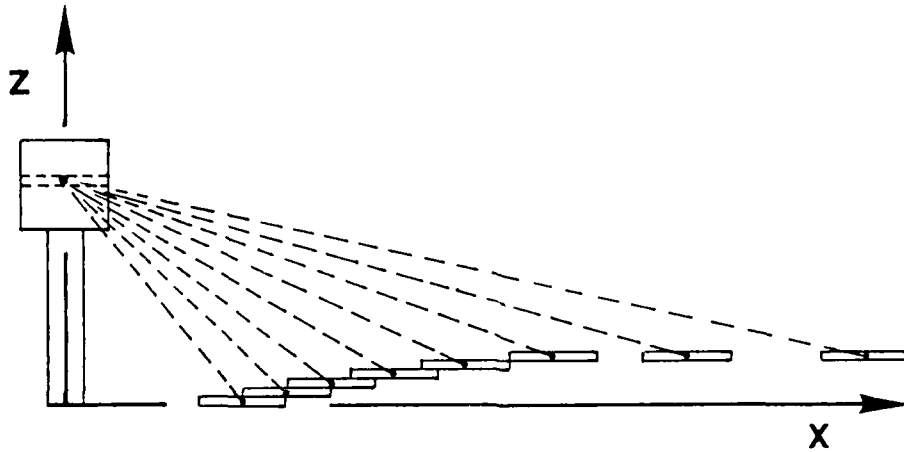
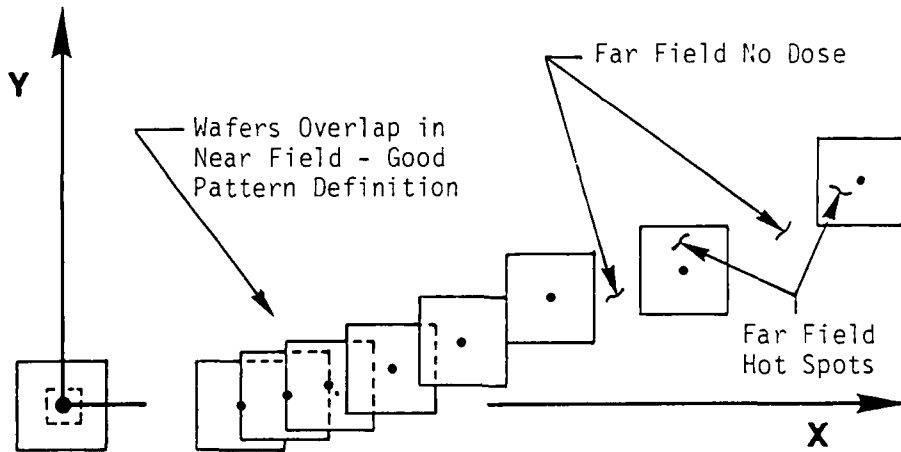


Figure 3.5 Particle Count as a Function of Size Classes and Wafers

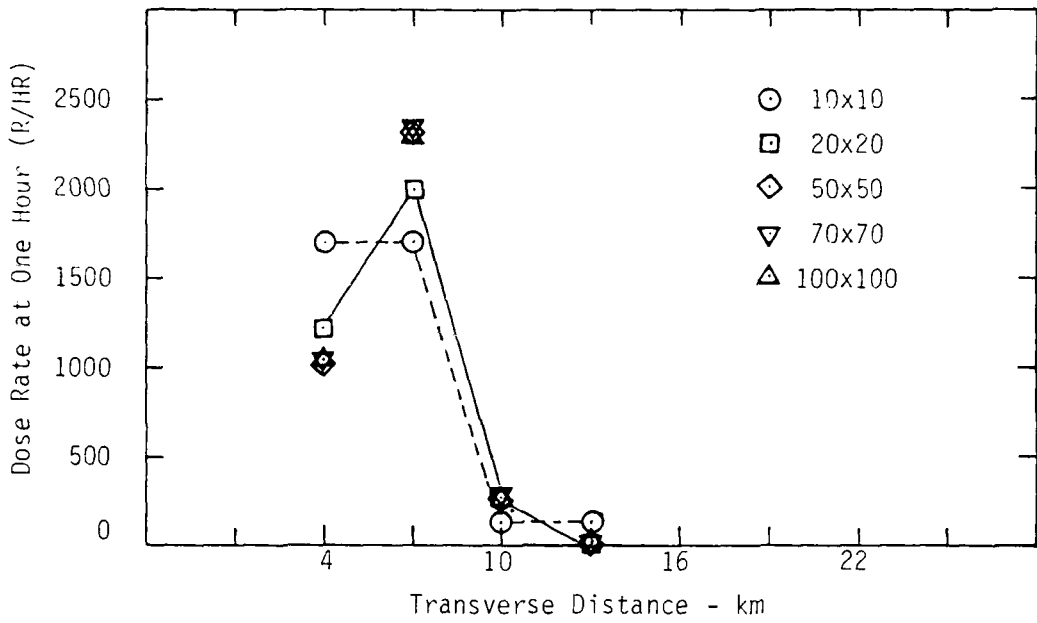


(a) Profile View - Trajectory of Different Size Classes From One Cloud Layer

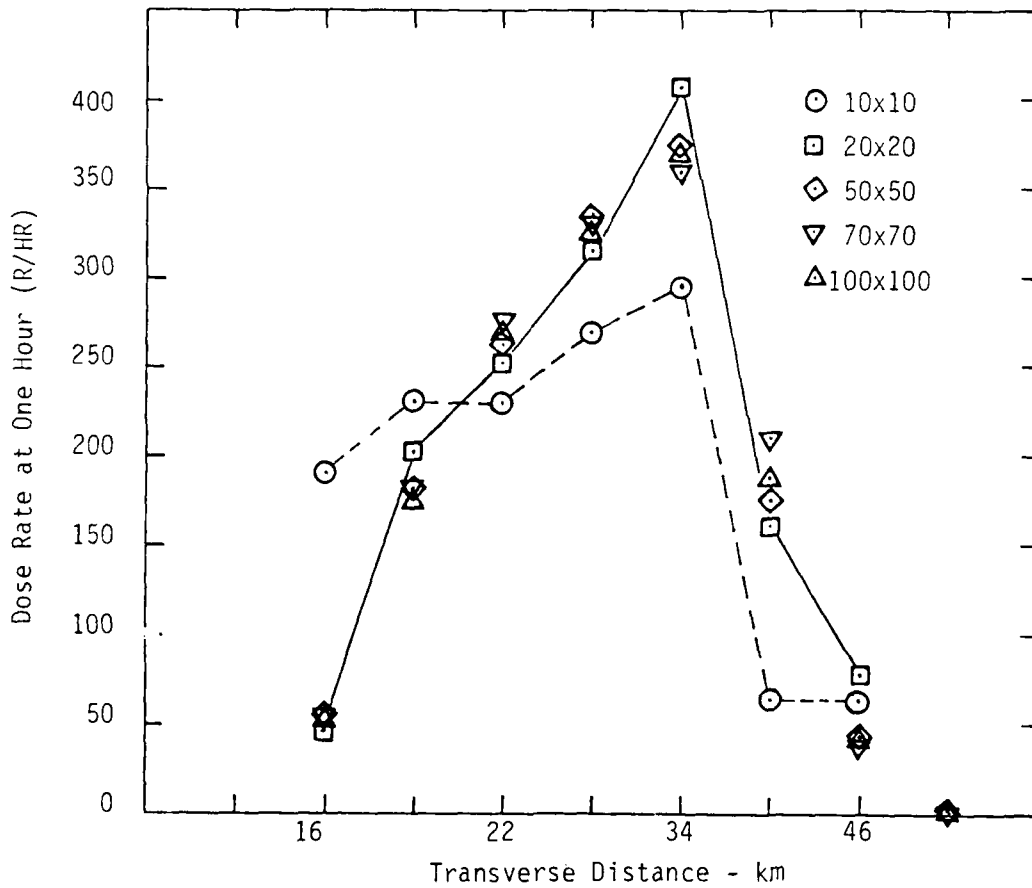


(b) Plan View of Part a - Wafers on Ground

Figure 3.6 DELFIC Field Definition From a Single Cloud Level

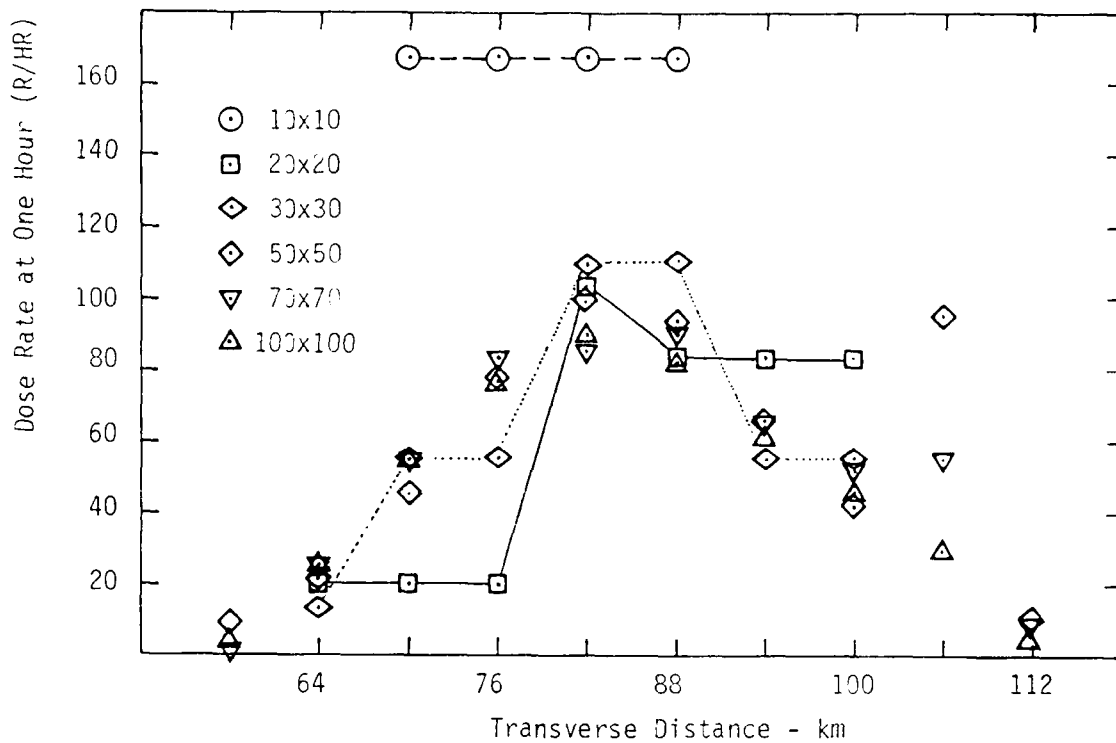


(a) 10 km Downwind

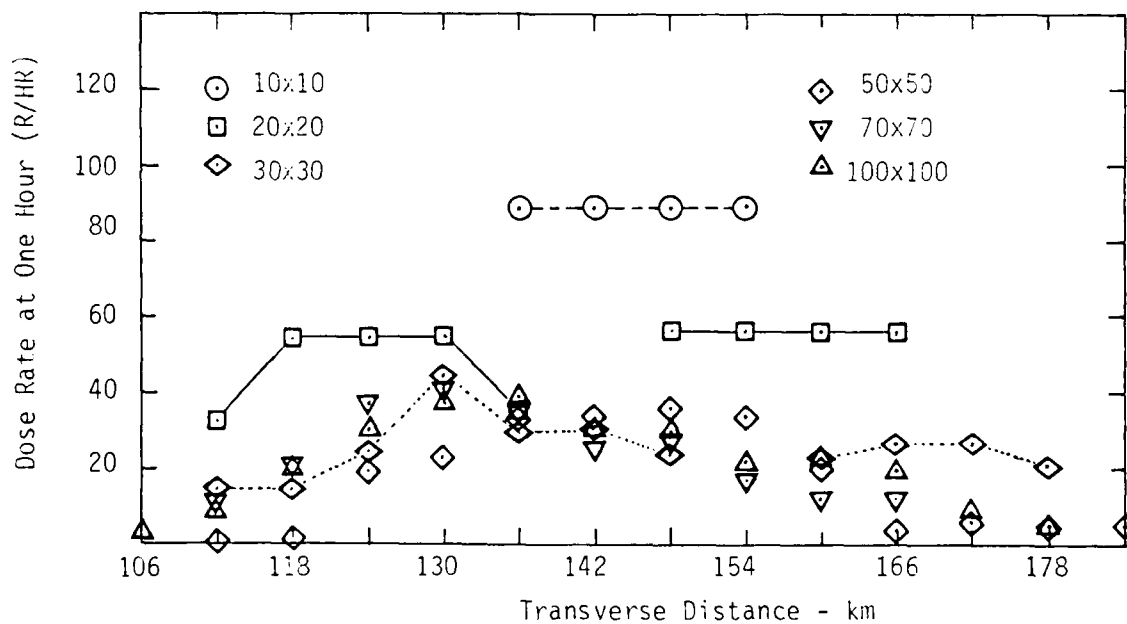


(b) 60 km Downwind

Figure 3.7 Downwind Transverse Dose Rate Distributions - 1 MT

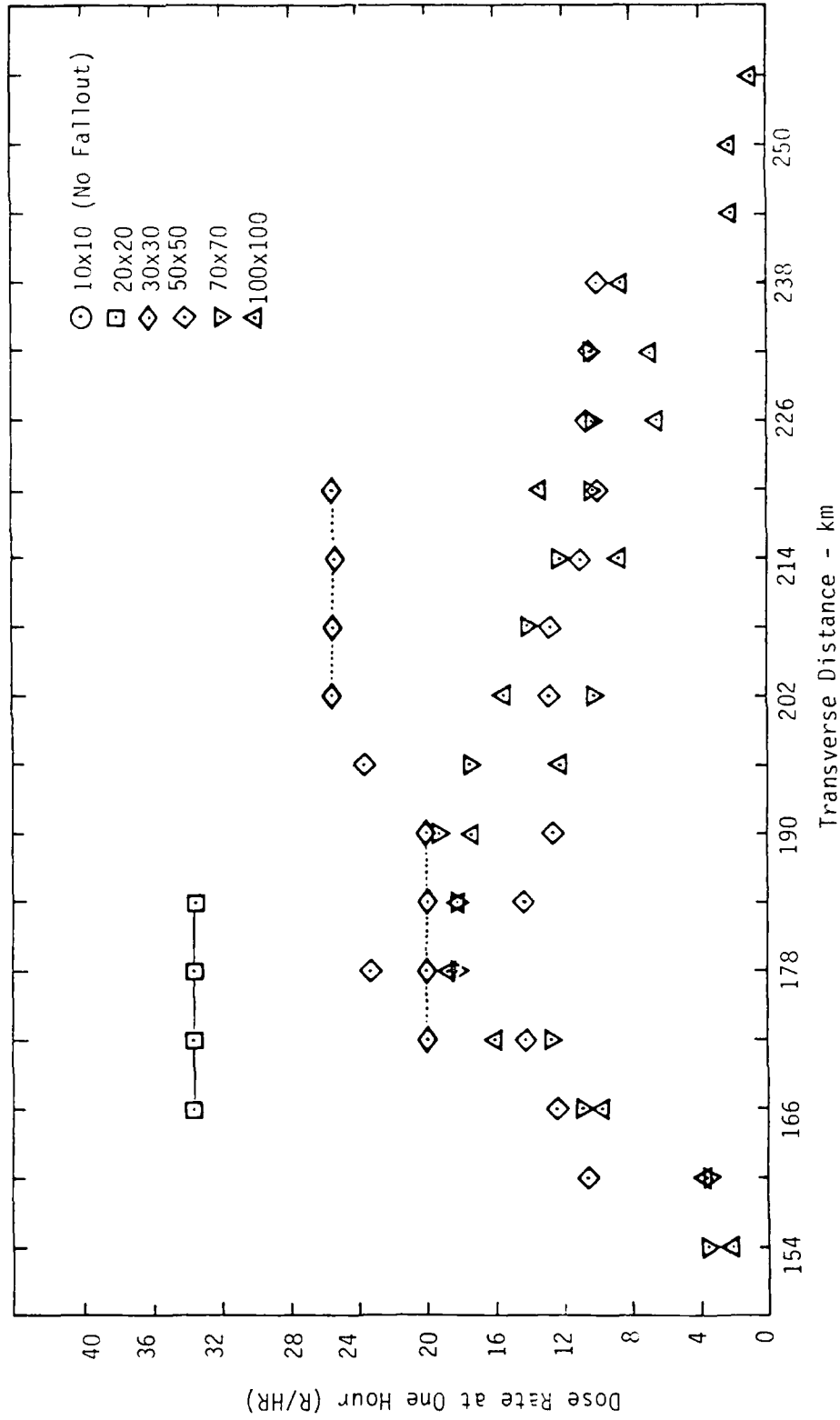


(c) 150 km Downwind



(d) 250 km Downwind

Figure 3.7 Downwind Transverse Dose Rate Distributions - 1 MT (continued)



(e) 350 km Downwind
 Figure 3.7 Downwind Transverse Dose Rate Distributions - 1 MT (continued)

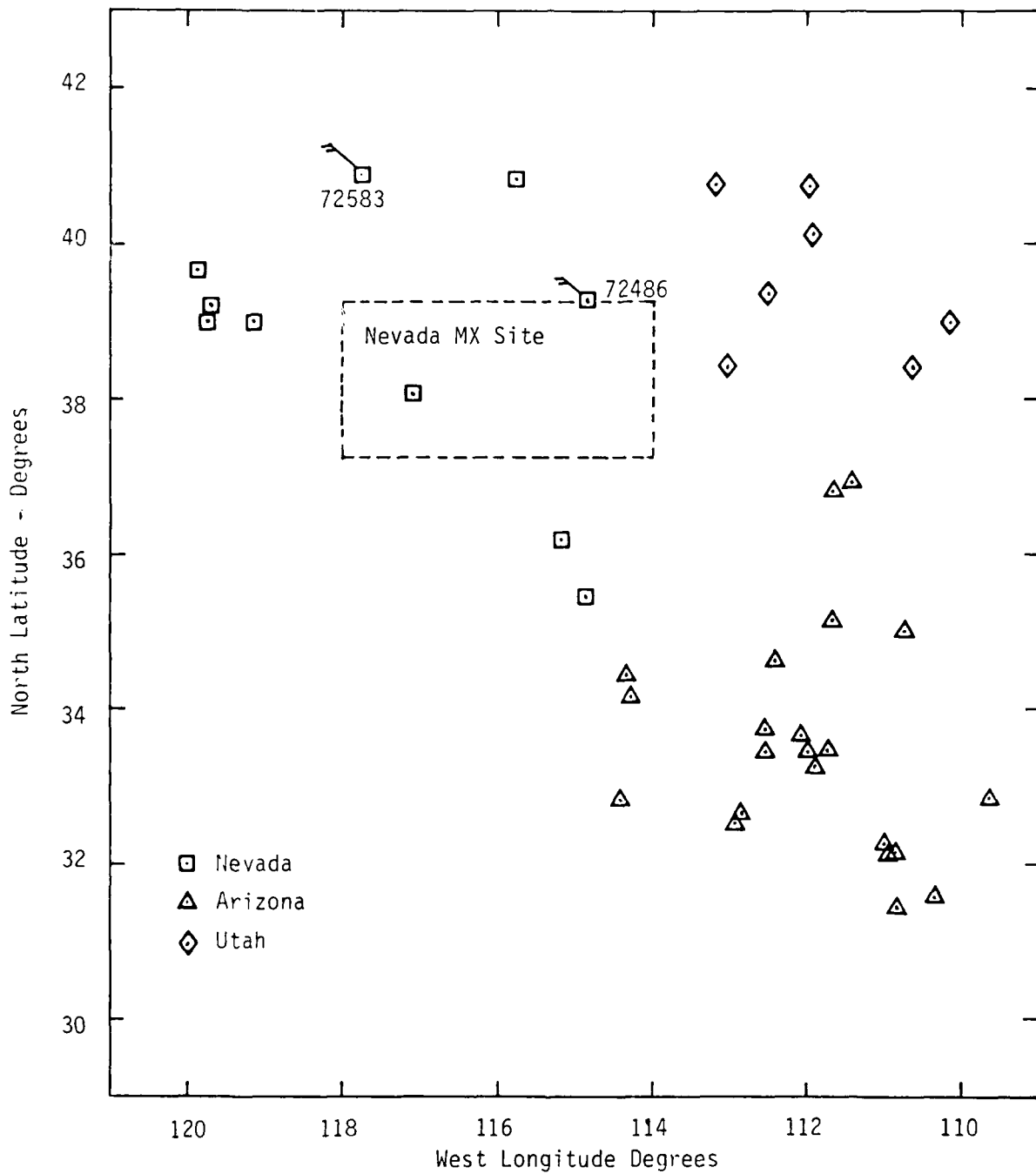


Figure 3.8 WMO Weather Stations Near Nevada MX Site

Section 4

POTENTIAL INTERACTIVE EFFECTS

In a single surface burst in the megaton range, the fireball gas (air and fission debris) is well mixed initially with crater material (i.e., dust). At about 5-10 seconds, the nuclear debris, in the form of a variety of radioisotopes, is condensing out onto whatever particulates are present. In the multiple burst case, it is reasonable to anticipate several anomalies in this mixing and condensation process. For example; shock-fireball interactions prior to the time of fission debris condensation might help separate the debris from the dust (particularly the larger particle sizes). The result would be seen in the activity-size distribution and possibly in the total activity in the close-in fallout. If there is a significant decrease in the activity on particles in the several hundred micron range, then one might expect a corresponding decrease in the on-site fallout.

The cloud rise and its stabilized altitude is also of concern in the multiple burst environment. The fireball rise could be different enough to affect the landing locations of large (>1mm) particles that fall out of the rising cloud. While not involving much of the total activity, the very close-in (several km) fallout would be affected. The stabilized height of the coalesced clouds will also affect the fraction of activity deposited on-site. For example, each 1 km difference in cloud height changes the range at which 100 μ particles land by about 25 km for a 30 knot wind.

The above illustrates the kinds of multiple burst effects that could impact the determination of how much fallout to expect on-site. In this section, we discuss briefly what has been learned from past investigations of interactions between bursts.

4.1 EARLY TIME MULTIBURST DUST CLOUDS

During an effort⁽⁴⁾ conducted earlier for Defense Nuclear Agency (DNA), SAI investigated the possibility of producing dust clouds from

multiple bursts that are potentially more severe than those obtained by adding dust densities using single burst models. Although the results of the assessment were preliminary, they showed that multiple-burst combined flow fields as predicted by LAMB* can enhance the dust density in some locations. In addition, for at least one case of strategic interest, the combined flow fields lofted more dust than would be lofted for the equivalent sum of single bursts. This observation was obtained by flying tracer particles through the LAMB-generated flow fields for two non-simultaneous 1 MT bursts detonating 2 kilometers apart. Burst times were different by 10 seconds. The performed calculations showed two effects: (1) the number of tracer particles lofted was increased for the first burst - apparently as a result of interactions of the shock from the second burst in the first's vicinity,** and (2) the additional dust remained in a fairly concentrated region giving rise to a high density pocket in the region where the stem for a single burst would have existed. The first effect can affect late time dust densities, whereas the second effect could increase the hazards of early time missile fly-out.

Figure 4.1 shows preliminary estimates performed for DNA of the dust cloud distribution for MX using flow fields from the LAMB model. The scenario considered was two surface bursts, separated spatially and temporally. The first burst was located at the origin, the second at 2 kilometers along the x-axis. Burst times considered were separated by 0, 2, and 10 seconds. The results are presented for two times, 20 and 40 seconds after the burst time of the first burst. The dust cloud is represented by tracer particles distributed about the first burst in an appropriate manner.

This figure clearly shows that multiburst dust environments cannot be represented by the simple addition of single burst clouds for early times. If they could, the dust cloud surrounding a burst would be independent of how many, where, or when any bursts occurred about it. If simple superposition worked, the dust clouds in Figure 4.1

* LAMB is the AFWL Low Altitude Multiple Burst Model (see Reference 5)

** The effect on tracer particles near the second burst was not investigated.

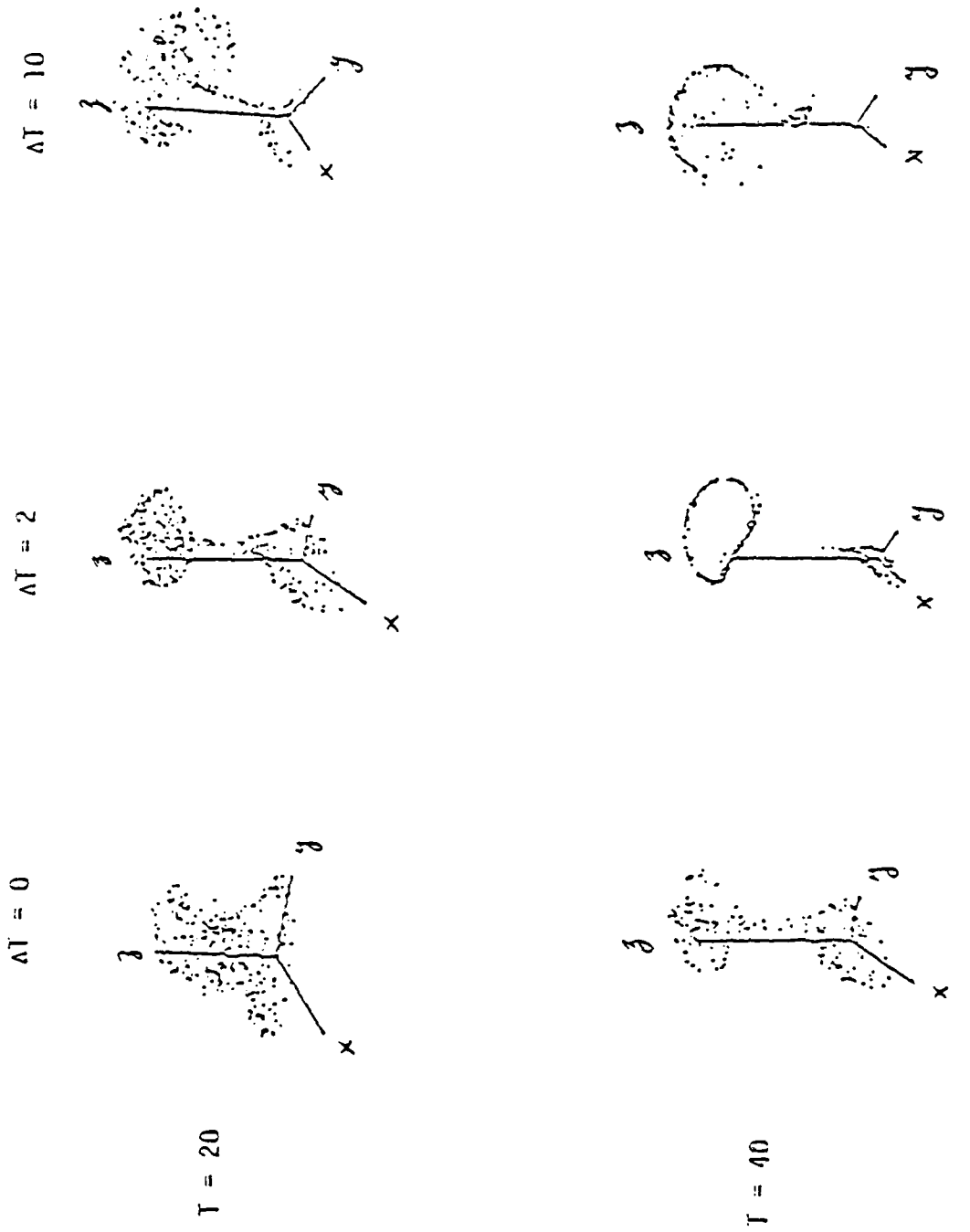


Figure 4.1 LAMB Tracer Particle Positions

for $T = 20$ seconds would be identical to one another as would those for $T = 40$ seconds. Since they are not identical and since there are cases where strong enhancement may exist, an effort⁽⁶⁾ to develop better algorithms for use in a multiburst dust environment was performed under subcontract to the McDonnell Douglas Astronautics Co. (MDAC) for a U.S. Army application.

In the effort for McDonnell Douglas, SAI performed two tasks related to nuclear multiburst phenomenology prediction. The first task was to develop algorithms for use in the MDAC Site Defense Low Altitude Multiple Burst Code (SD-LAMB) to permit the generation of dust clouds including the stem, cloud and skirt during interactive multiburst scenarios anticipated in the defense of the U.S. Air Force M-X weapons system. The second task, a much smaller effort than the first, was to investigate whether it is desirable to modify LAMB burst generation for detonations inside previous fireballs. The details of the investigation can be found in reference 6.

However, the efforts described above in no way were intended to produce definitive models to assess satisfactorily what the significance of multiburst effects are to fallout. Nevertheless a brief review is presented of the effects (as predicted by the LAMB code) that a shock wave from a burst has on a neighboring burst's fireball development. Various results from SAI LAMBDA* calculations performed for this effort are also presented and discussed.

The effect of the shock of one burst on the flow field of another affects the latter's fireball development. This effect is less pronounced for separations much greater than 2 km. Figure 4.2 shows the trajectory of one of the fireball centers for three cases: one undisturbed burst, two bursts separated by 2 km, and two bursts separated by 4 km. The multiburst cases were for simultaneous detonations. The hash marks along the trajectories correspond to time in

*LAMBDA is an SAI code that flies dust through a LAMB-generated multiburst flowfield.

7

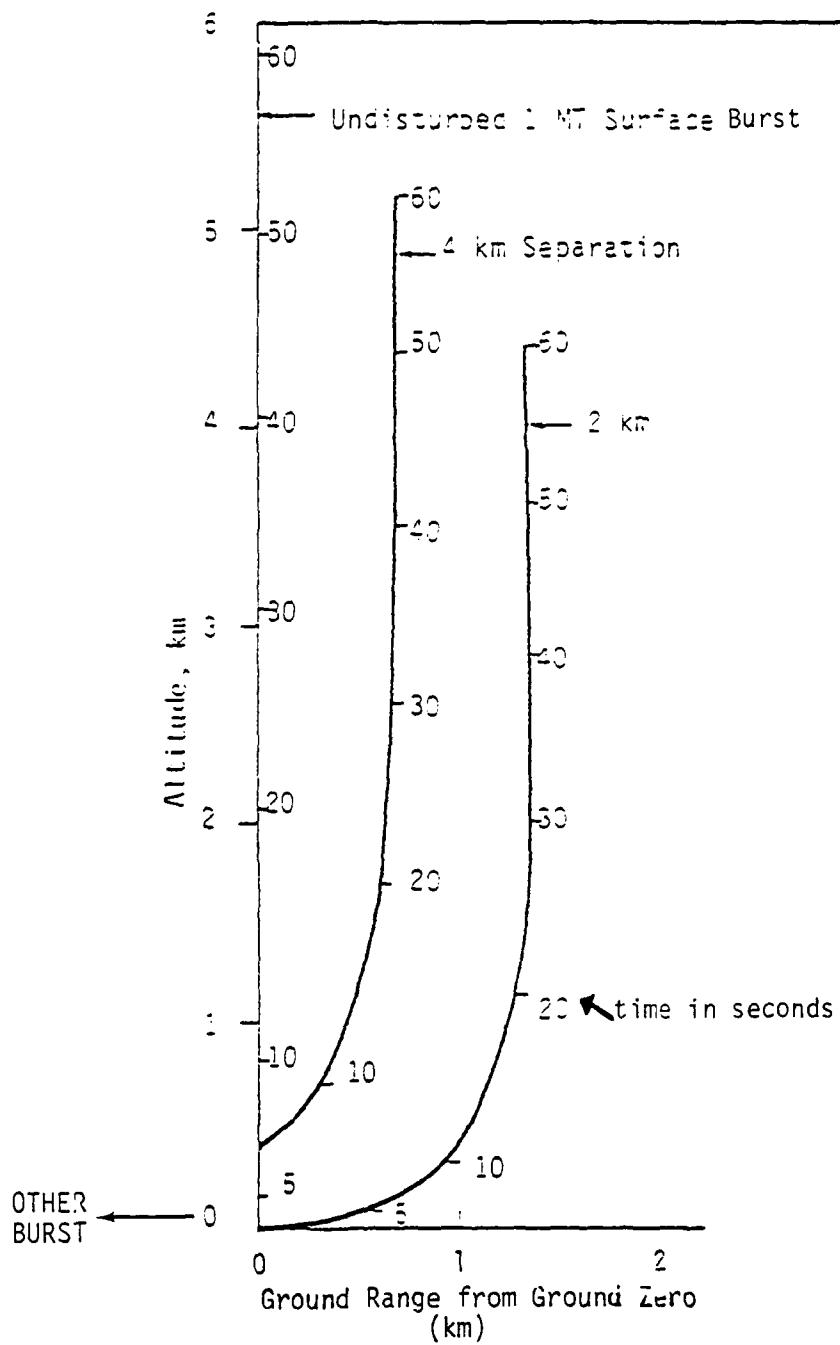


Figure 4.2 Comparison of Multiburst Shock Effects for Several Double Burst Separations

seconds. For bursts as close as 1 kilometer the LAMB algorithms lead to an almost immediate combining of the fireballs, which is not shown in the figure. Combining causes the fireballs to move towards, rather than away, from one another.

The LAMB multiburst shock effects on early-time fireball trajectories vanish when the two simultaneous 1 MT bursts are separated by more than 8 km. This is obvious from Figure 4.3 which presents the direction of the velocity vector of the fireball center immediately after shock arrival. From inspection of Figures 4.3 and 4.4, it is evident that for spatial separations exceeding 8 km the predicted effects of early time multiple-burst interactions between 1 megaton bursts is small.

Finally, the effect of the shock on fireball size as modeled by LAMB is not very significant. This is shown in Figure 4.5 for a 2 km separation. Two radii are plotted in this figure: that transverse to the velocity vector of the fireball center, and that parallel to it. The position of the fireball (and its direction of travel) will greatly influence the LAMB-modeled flow fields. These in turn will affect the transport of the dust.

4.2 STATUS OF MULTIPLE BURST INVESTIGATIONS RELATED TO MX

The above discussion focussed on 2 bursts occurring close in time and/or space. An attack on MX, however, is postulated to involve perhaps thousands of bursts. Hence, simple algorithms based on 2-burst calculations cannot be assumed to be valid.

To address the issues pertinent to MX, two activities have been undertaken. One is a series of calculations by AFWL using the HULL code.* The first of these was a two-dimensional calculation of 60 bursts arranged in concentric rings. Interactions were accounted for between rings but

* HULL is a computer code that performs two-dimensional and three-dimensional hydrodynamic calculations (see for example references 7 and 8).

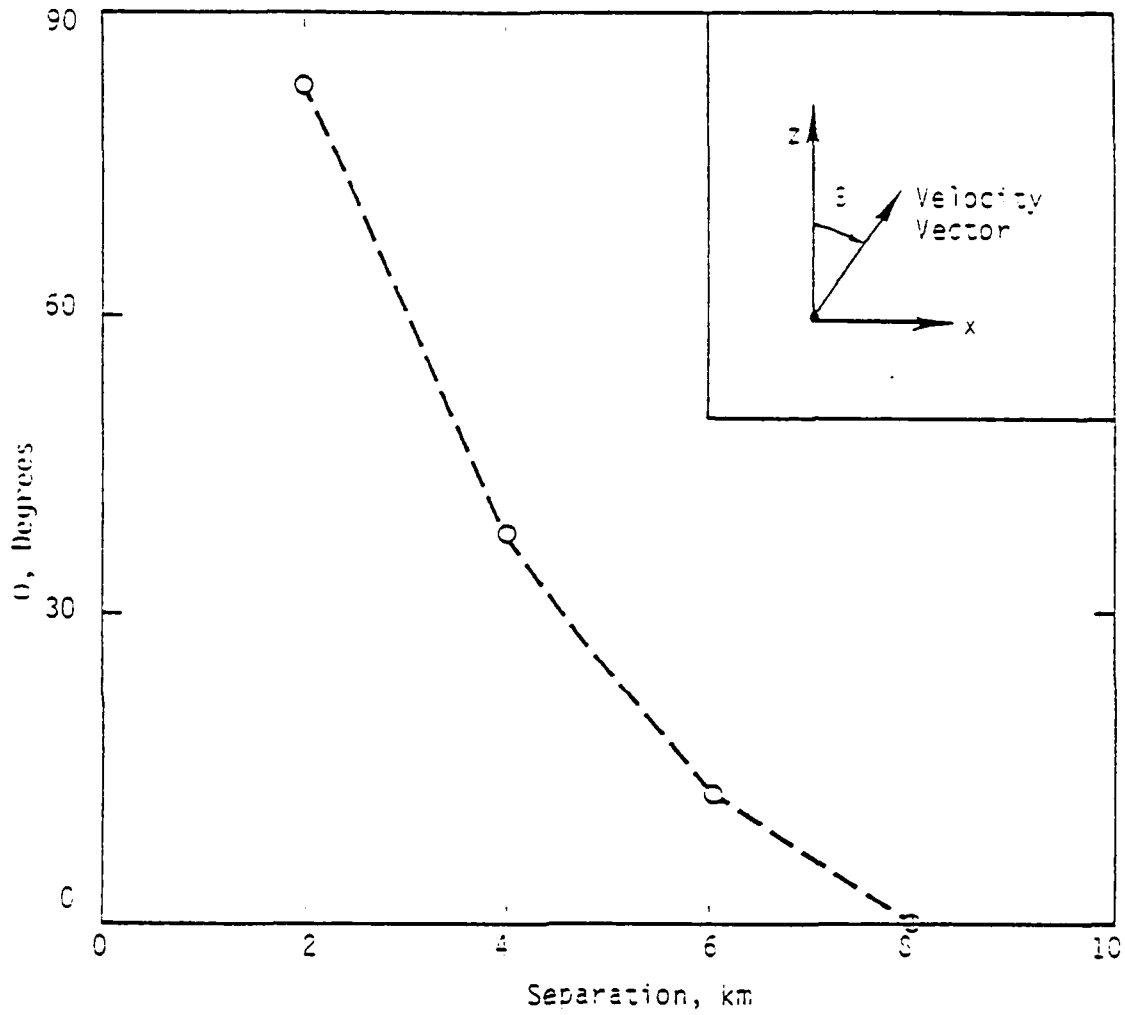


Figure 4.3 Direction of Velocity Vector of Fireball Center Immediately After Shock Arrival, As a Function of Burst Separation, For Two Simultaneous 1 MT Bursts

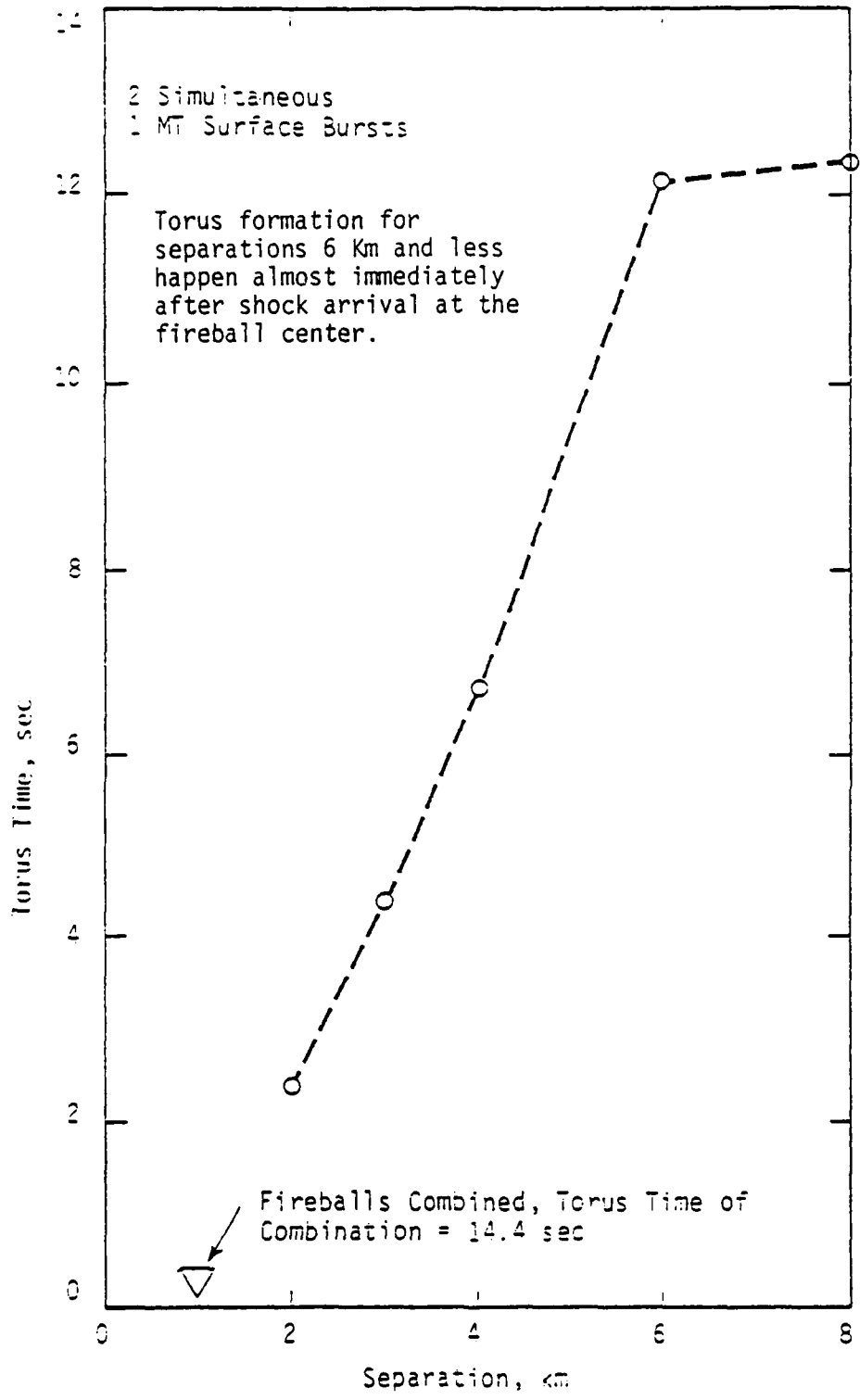


Figure 4.4 Torus Time for Different Burst Separations

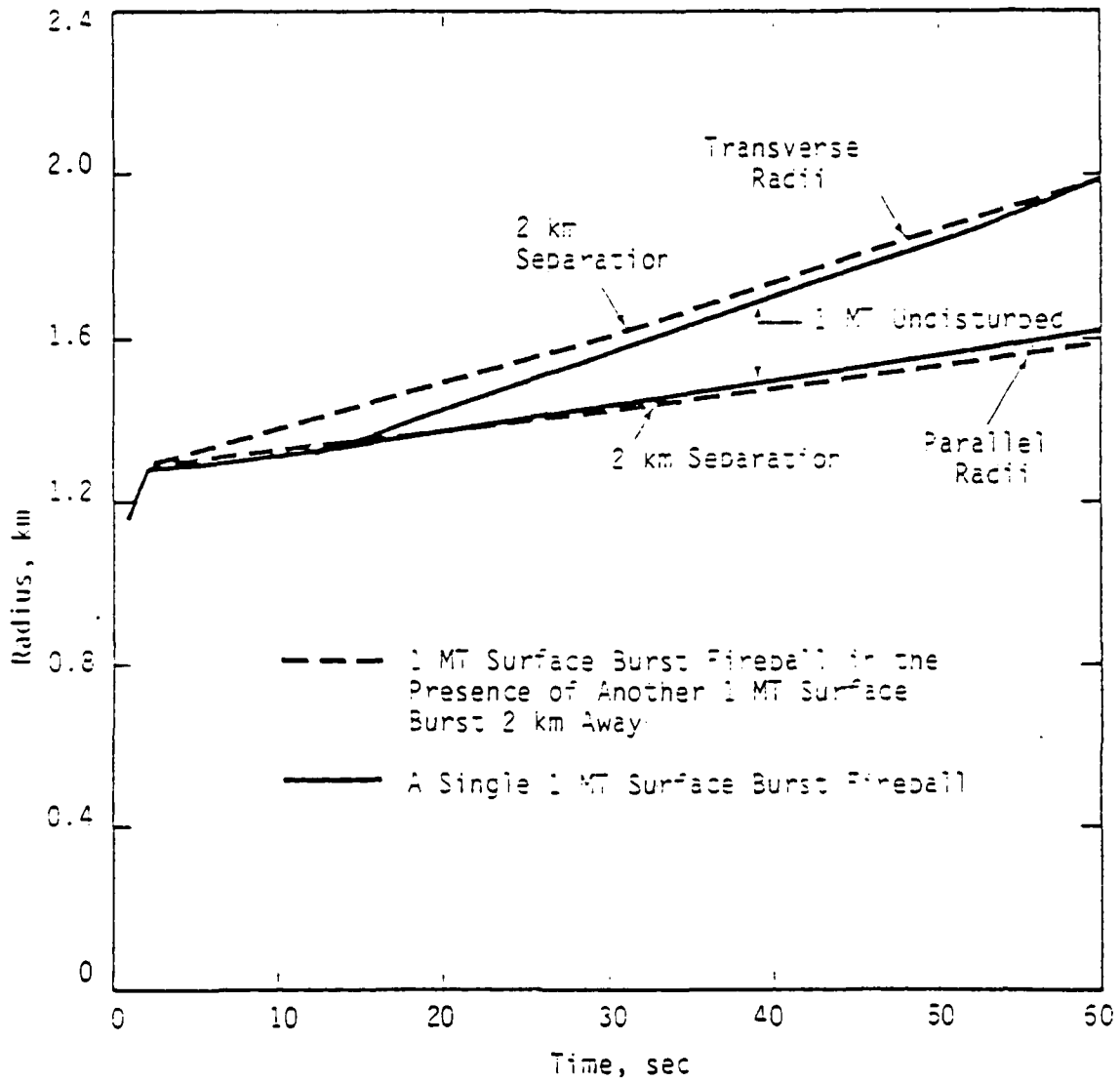


Figure 4.5 Fireball Growth (Single Burst Versus Multiple Burst)

not between bursts in the same ring. Anomalies in cloud rise relative to a single burst were noted. However, until this two-dimensional synthesis used can be demonstrated to be valid (i.e., with a full three-dimensional calculation), these rise anomalies cannot be incorporated into the assessment of on-site fallout. Results from the 3-D calculations are not expected for about 6 months.

In addition to the above, there was recently a simulation of multiple bursts using six 120 ton high explosive charges. This experiment, called MISERS BLUFF II-2, produced results on cloud geometry and particle size distributions. Analyses of these measurements are currently underway and are expected to provide validation of the calculational results discussed above.

In summary, then, the status of the multiple burst calculational and simulation programs does not, at this time, permit credible modifications to the assumption of superposition in the assessment of on-site fallout.

SECTION 5

RESULTS

5.1 TYPICAL RADIATION LEVELS

This section presents the fallout calculations performed for the laydown discussed in Section 2. The cumulative dose rate from all contributing bursts is determined at each of 177 monitor points on the Nevada model site. By and large these monitor points are uniformly spaced so that the number of monitor points receiving a given dose rate may be considered equivalent to the fraction of the total site area receiving that dose rate. Figures 5.1 and 5.2 show the physical placement of these monitor points within the land parcels described in Section 2. The number at each of the monitor points is the dose rate at H+1 hour in thousands of R/Hr. Lower dose rates occur along the upwind periphery because fewer bursts are contributing to the fallout arriving at those sites. These figures represent the distribution of fallout intensities for two of the wind samples used in this study. They were chosen only to illustrate the general characteristics of the distribution over the deployment area under consideration.

5.2 IMPACT OF WIND VARIATION

As discussed in Section 3, 40 wind samples were selected with 10 per quarter and an explicit calculation of the fallout was done for each. For each wind sample, a dose-rate distribution curve was constructed. Figures 5.3 through 5.6 show these distributions by quarter. The abscissa of these plots is defined as the fraction of monitor points (or site area) for which the dose rate was at least that indicated. If, for example, the curve coordinates were 10 percent and 100,000 R/Hr, then 10 percent of the site area received at least 100,000 R/Hr. As can be seen in each of these figures, there is considerable variation from one wind sample to another. In the first quarter, for example, the median dose rate (i.e., corresponding to 50 percent in the area

covered) varies from 24,000 to 66,000 or almost a factor of 3. For 10 percent of the area, the minimum dose rate varies from 55,000 to 105,000 R/Hr which is about a factor of 2. Note that this wind variability as evidenced by the variability in the curves, increases to a maximum for the fourth quarter where the median dose rate ranges over a factor of 4. The envelope of distribution curves for all 4 quarters and the annual average dose rates for 10 percent and 50 percent of the area are presented at Figure 5.7. Table 5.1 summarizes the seasonal variation in the median dose rate as well for the tenth percentile dose rate. Note that the third quarter averages are the highest. As indicated by the standard deviations, however, the scatter within a given quarter makes the seasonal variations just barely significant. Finally, for all 40 wind samples, the average of the median dose rate is 55 ± 21 K R/Hr and the average of the tenth percentile dose rate is 96 ± 27 K R/Hr.

5.3 ACTIVITY AND MASS DEPOSITED ON SITE

As a matter of interest, computations were made to determine the percent of activity and mass deposited within the nominal boundaries of the deployment site. The day selected for the illustrative computation was one associated with heavy fallout, i.e., low wind speeds which result in heavy deposition of radioactive material on monitor points. Calculation showed that for such conditions, the ratio of activity deposited on site with respect to the total produced in the 3538 weapon attack was 0.46. Similar calculations for mass showed that the percent of on-site deposition was 0.53. The differing values for activity and mass deposited are a reflection of the non-uniform distribution of activity with particle size.

5.4 OPERATIONAL IMPLICATIONS

Some of the operational implications of the fallout hazard can be taken from Figure 5.8, which displays parametrically several combinations of transmission factors and stay times which can be correlated with entry times and levels of radiation. The allowable dose for personnel was assumed to be 100 RAD in all cases, a value which is normally equated to the emergency risk level in military operations. By referring to this figure, the user can inspect a broad range of possible conditions that may have to be considered in terms of both system design (e.g., transmission factors) and tactical considerations such as allowable delay from initial attack until repair crews could enter the contaminated area.

5.5 RADIATION ARRIVAL TIMES AND PERSISTENCE

Figures 5.9 through 5.13 of this section show the time history of radiation rates for 5 monitor points selected from various locations in the proposed deployment area. As expected, they exhibit the usual pattern -- rapid initial buildup to peak value followed by exponential decay. It is interesting to note that the peak intensities occurred prior to H+1 hour, usually at or just under H+30 minutes. This is a result of a number of factors, including the 7000 foot separation of sites, the attack pattern, the winds, the particle size distribution used in DELFIC and the yield of attacking weapons. The total unshielded dose for any given time period is the area under the curve in that time interval. The rates of decay at slopes less steep than the "standard" $t^{-1.2}$ are reflections of the fact that DELFIC has some particles arriving after H+1, contributing to the dose rate and thereby slowing overall decay. This deviation from the standard $t^{-1.2}$ decay law assumption points up the need for in-place, real time radiation monitor devices to acquire timely and accurate information on the intensity of the radiation hazard throughout the deployment area. It may well be that significant numbers of missiles will survive the

prompt effects of the attack and require some form of repair to be returned to operational status. In that event, preattack estimates of the hazard will not be adequate for the determination of radiation levels, and retaliation response times may require prompt action. If these conditions exist, an in-place radiation monitor system would be invaluable.

5.6 SYSTEM DESIGN CONSIDERATIONS

The technical results of this brief study have a host of both design and operational implications for the MPS deployment of IIX. There is an obvious need to ensure that the design is "balanced" from at least two different standpoints. First, although it is not within the scope of this study, there is a need to achieve design balance in terms of system response to the prompt versus residual nuclear effects of the attack. This will require an assessment of the threat from prompt effects to ensure that design steps to counter the radiation hazard are not rendered meaningless, i.e., if the blast and ground shock threat of Soviet offensive systems to the proposed IIX deployment is extremely high, it may be futile to expend resources to protect the system from fallout. Second, when one examines the hazard solely from the fallout standpoint, it is clear that there must be a balance of design protection for electronic equipment versus personnel. At this point, it appears that personnel vulnerability may be the more serious constraint. However, the simple fact of availability of data defining degrees of vulnerability of equipment versus personnel enables consideration of a variety of design configurations in terms of launch point shelter, on-site sensors, need for manual operations, command and control, and logistics.

5.7 ALTERNATIVES IN ASSESSMENT

The reader is reminded that the results of this report are those associated with a high-intensity attack involving 3538 surface burst one-megaton weapons, and arriving simultaneously at the targeted launch points. It may be relevant to consider some forms of limited attack and the resultant radiation hazard associated with them. Alternatively, it may be useful to examine some variations in launch-point spacing and pattern which present fratricide problems for the attacker while diluting the attack intensity in terms of weapons per unit area, thus reducing the fallout radiation hazard. In any event, final decision on system feasibility will necessarily require an analysis and comparison of alternative designs. In the absence of specific criteria for equipment hardness, launch window requirements, entry and staytime guidelines, etc., the parametric approach to assessment of the radiation hazard appears most appropriate -- at least initially. Figure 5.8 provides one example of how key factors can be parameterized.

5.8 UNCERTAINTY PERSPECTIVE

The quarterly dose rate distributions over the 177 monitor points shown in Figures 5.3 through 5.6 provide some definition of the uncertainty associated with the quantification of the fallout hazard, i.e., the range of dose rates that may occur simply as a function of wind variation. Clearly, there are other uncertainties of significance -- cloud height variation for example, and other factors that may deviate from "standard" assumptions as a result of the interactive effects attendant to an attack of closely-spaced, high yield weapons such as the one examined here. No attempt was made to analyze and correlate these uncertainties exhaustively in the course of this study. Rather, the effort was directed at providing the best estimate of the hazard based upon consideration of the variables generally thought to be of greatest importance, e.g., attack pattern, intensity, fission fraction and wind variation. If, in SAMSO's judgment, there is justification

for further refinement of the estimate, some additional uncertainty analysis should be done to ensure that the bounds of the hazard have been defined adequately.

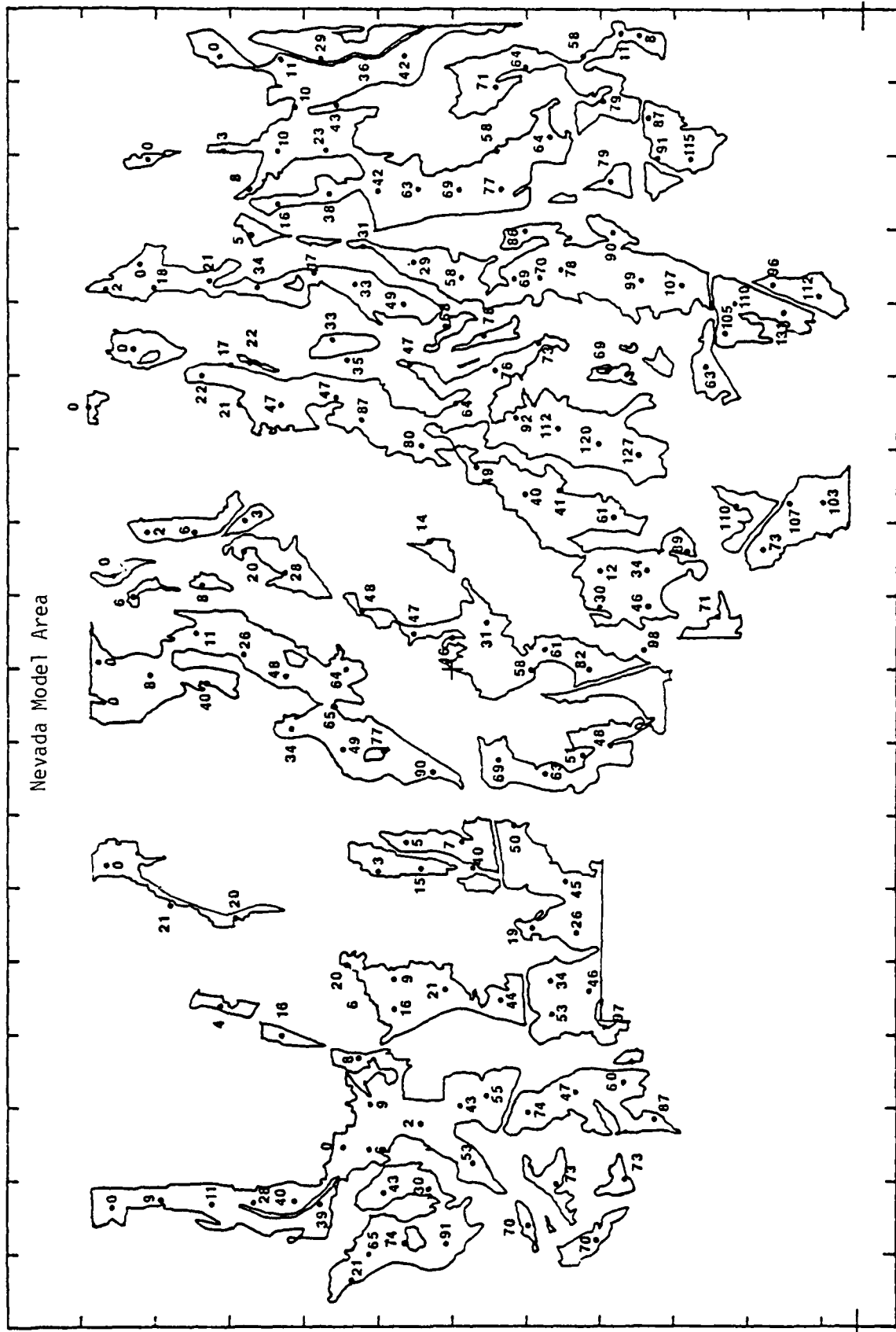


Figure 5.1 H+1 Hour Dose Rate Distribution, Moderate Wind Case. Dose rates are in Kilorads/hour.

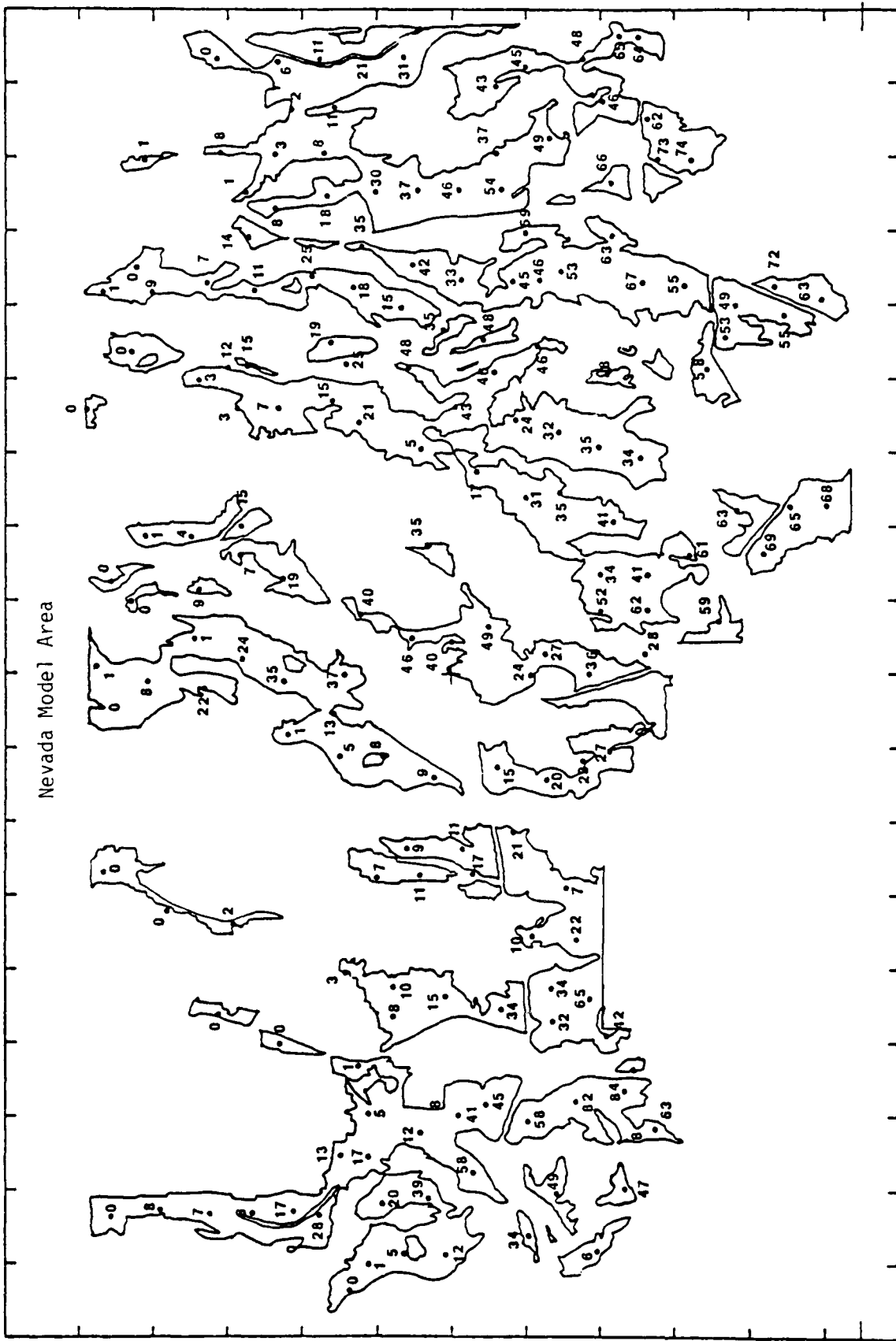


Figure 5.2 H+1 Hour Dose Rate Distribution, High Wind Case. Dose rates are in Kilorads/hour.

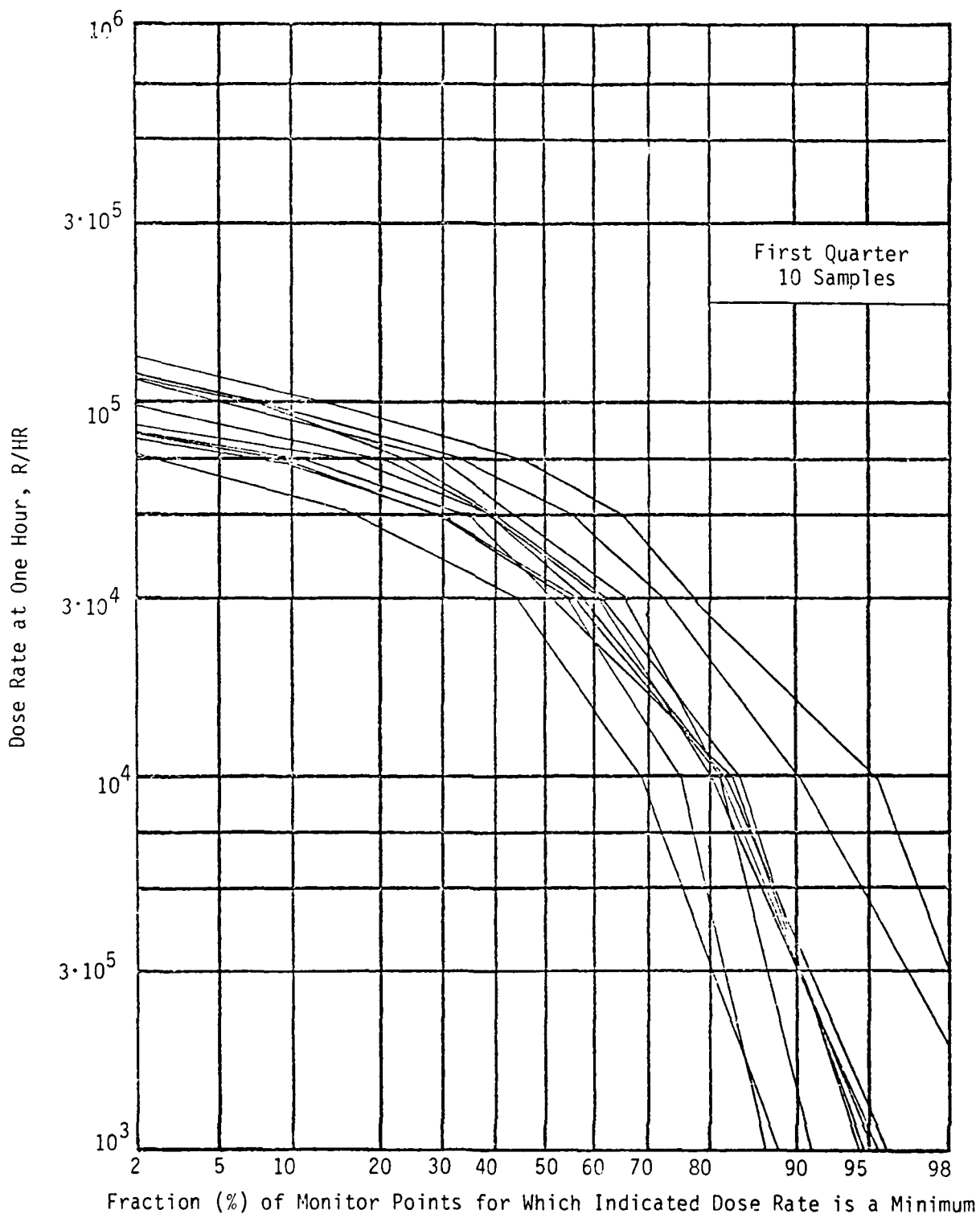


Figure 5.3 Dose Rate Distribution, First Quarter

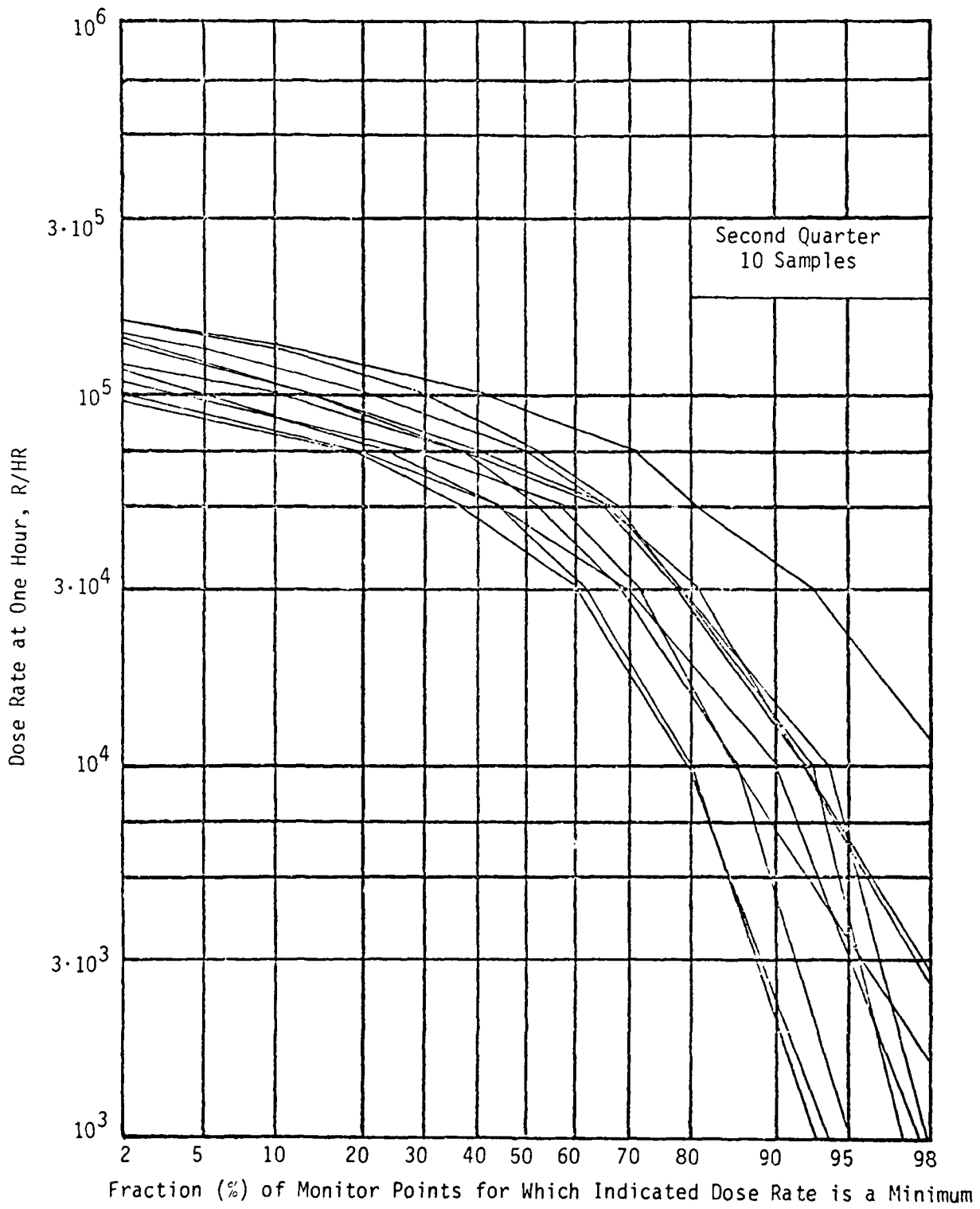


Figure 5.4 Dose Rate Distribution, Second Quarter

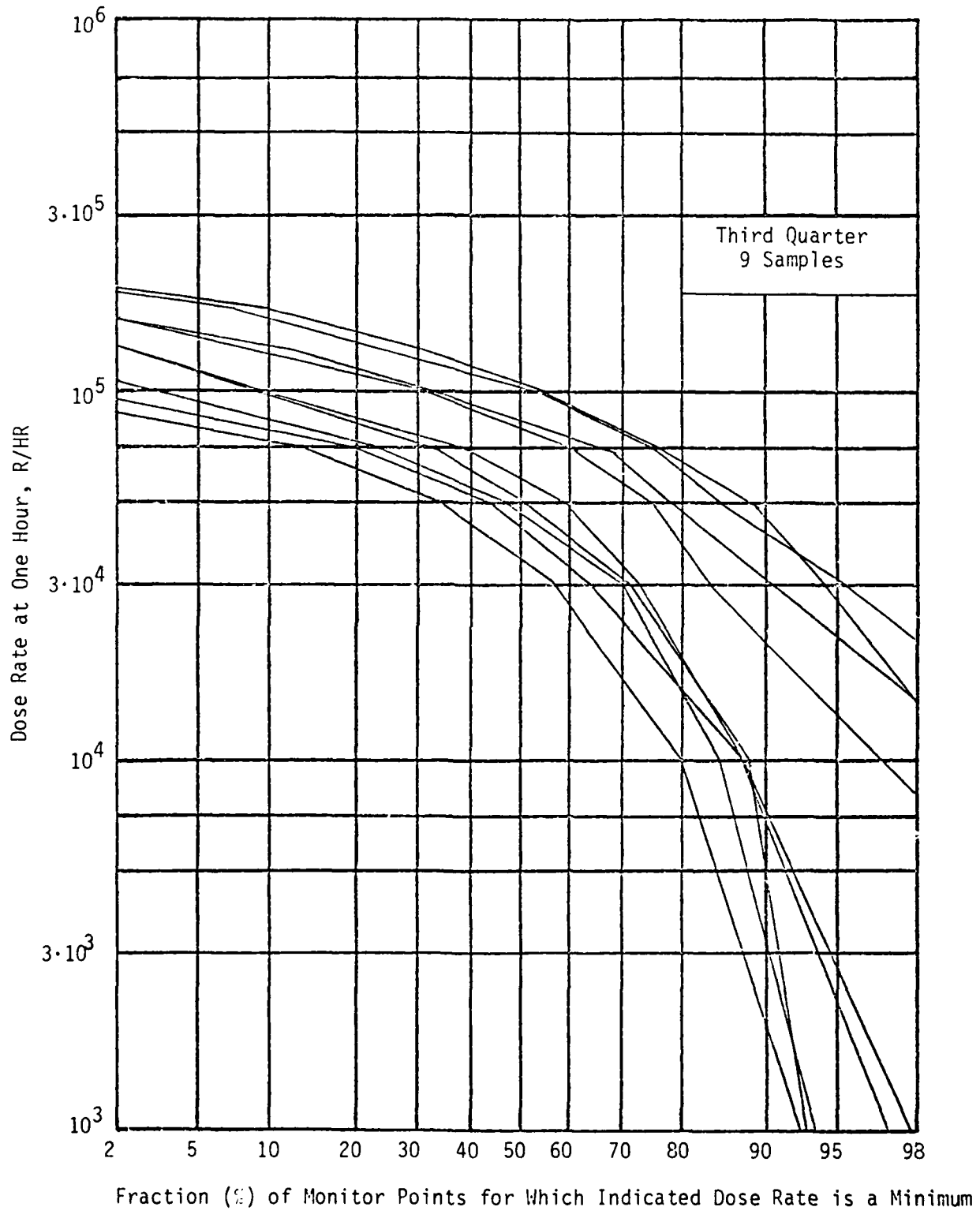


Figure 5.5 Dose Rate Distribution, Third Quarter

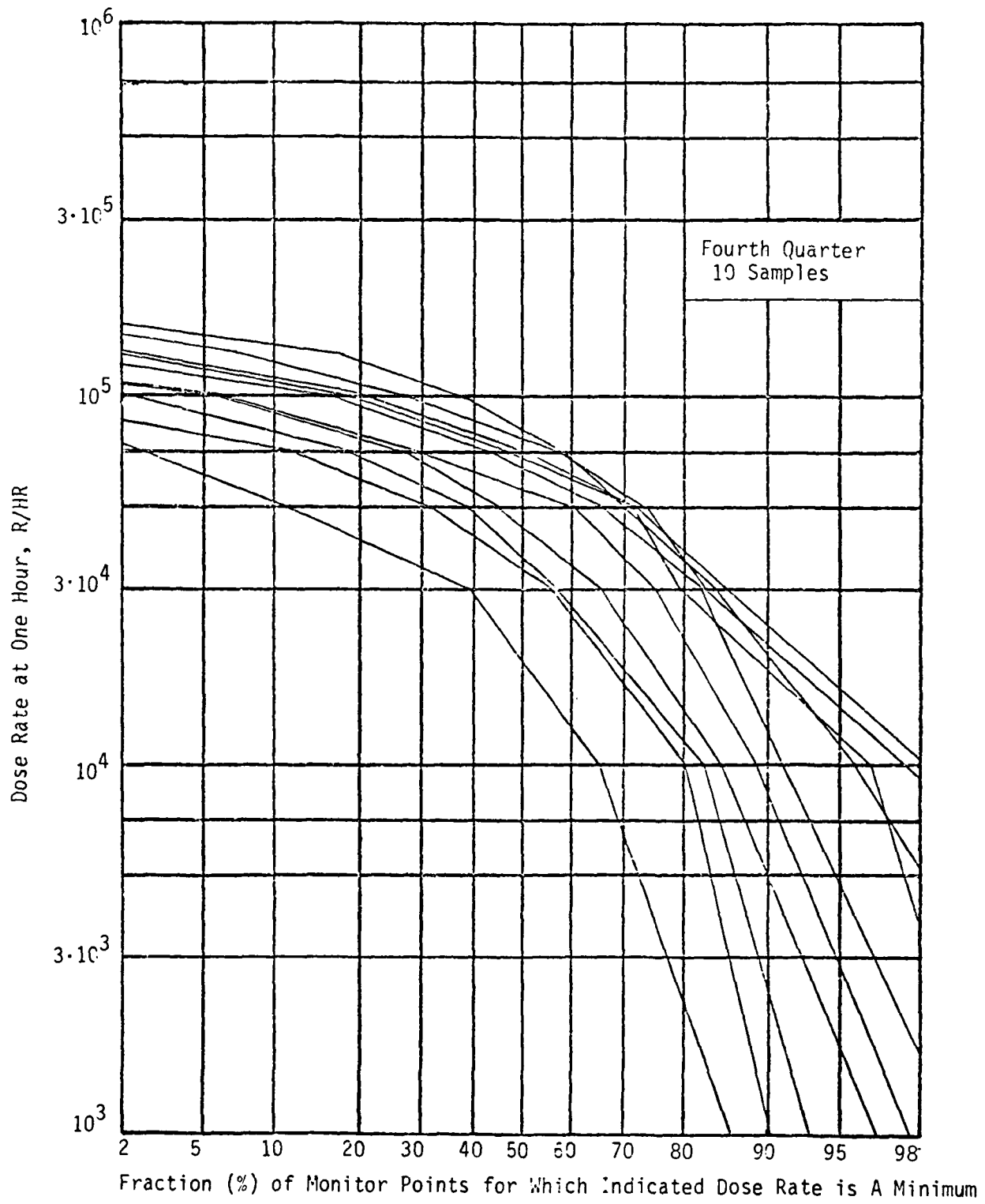


Figure 5.6 Dose Rate Distribution, Fourth Quarter

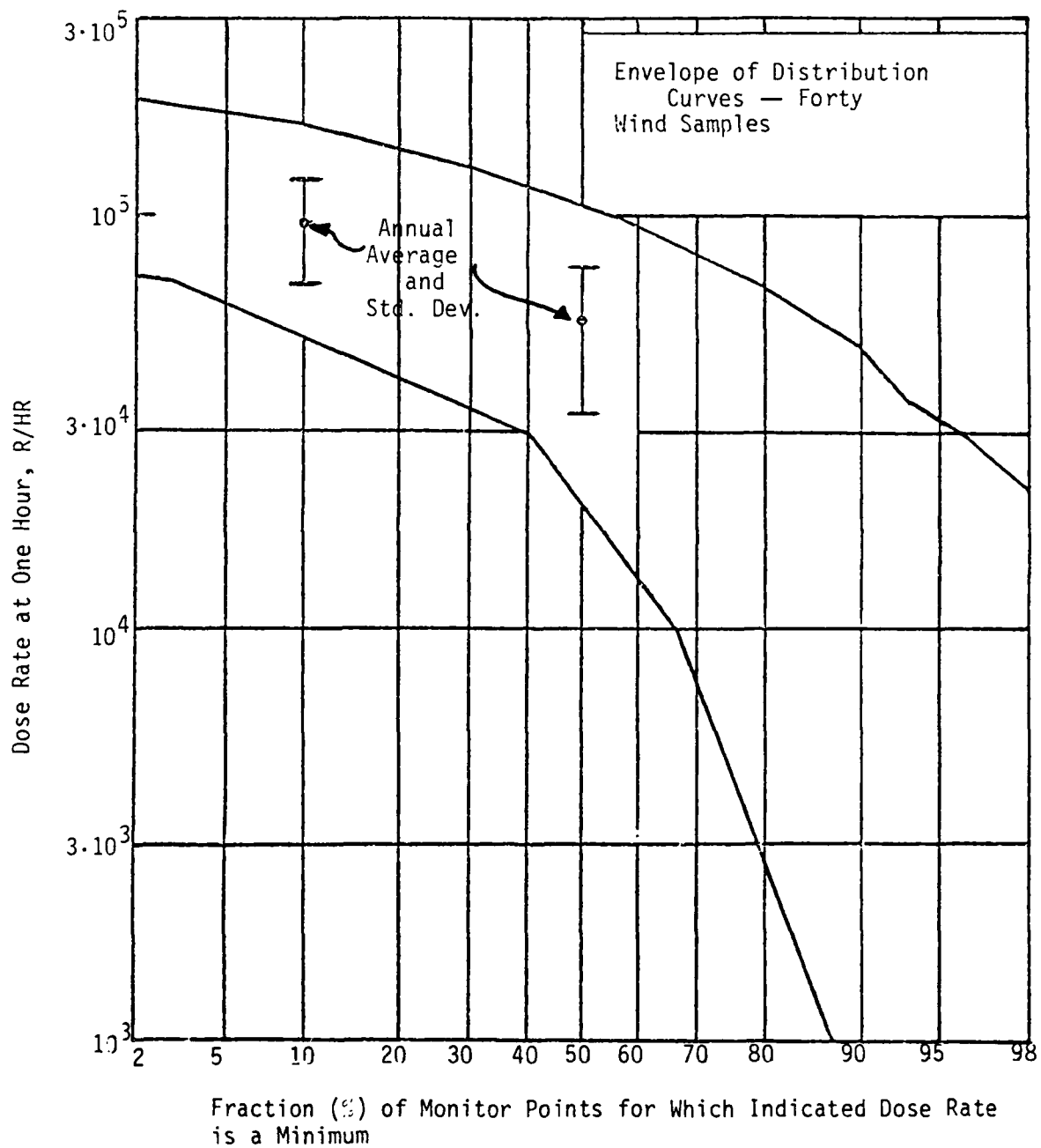


Figure 5.7 Annual Envelope of Dose Rate Distribution, Forty Wind Samples

QUARTER	DOSE RATE AVERAGE	
	10%*	50%*
1	80 ± 16 KR/HR	41 ± 12
2	102 ± 22	58 ± 16
3	113 ± 34	68 ± 27
4	97 ± 25	56 ± 21
ANNUAL	96 ± 27	55 ± 21

* Percent of monitor points for which indicated dose rate is minimum

Table 5.1 Dose Rate Distribution Summary

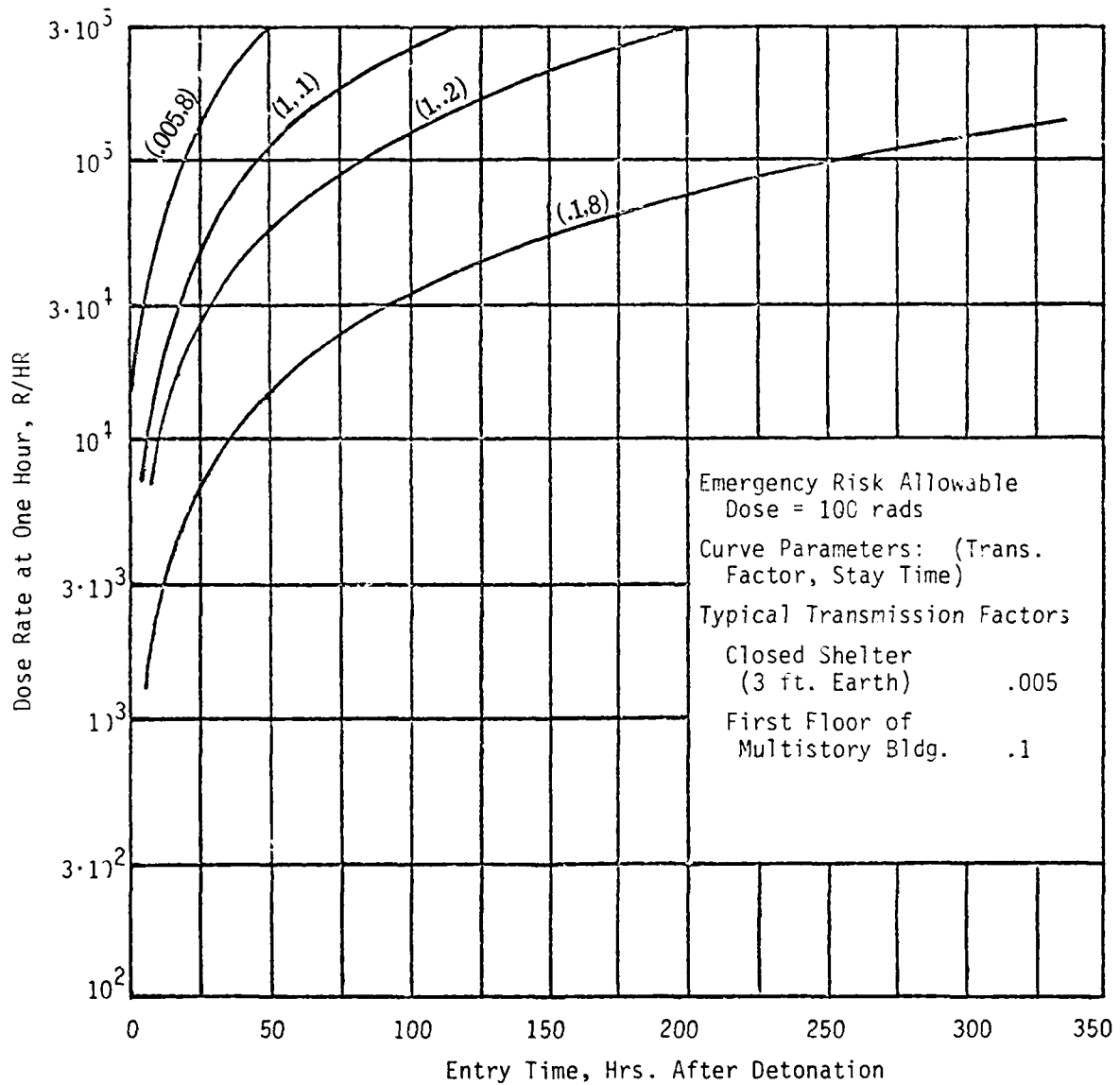


Figure 5.8 Parametric Assessment of Fallout Hazard, 100 Rads Allowable Dose

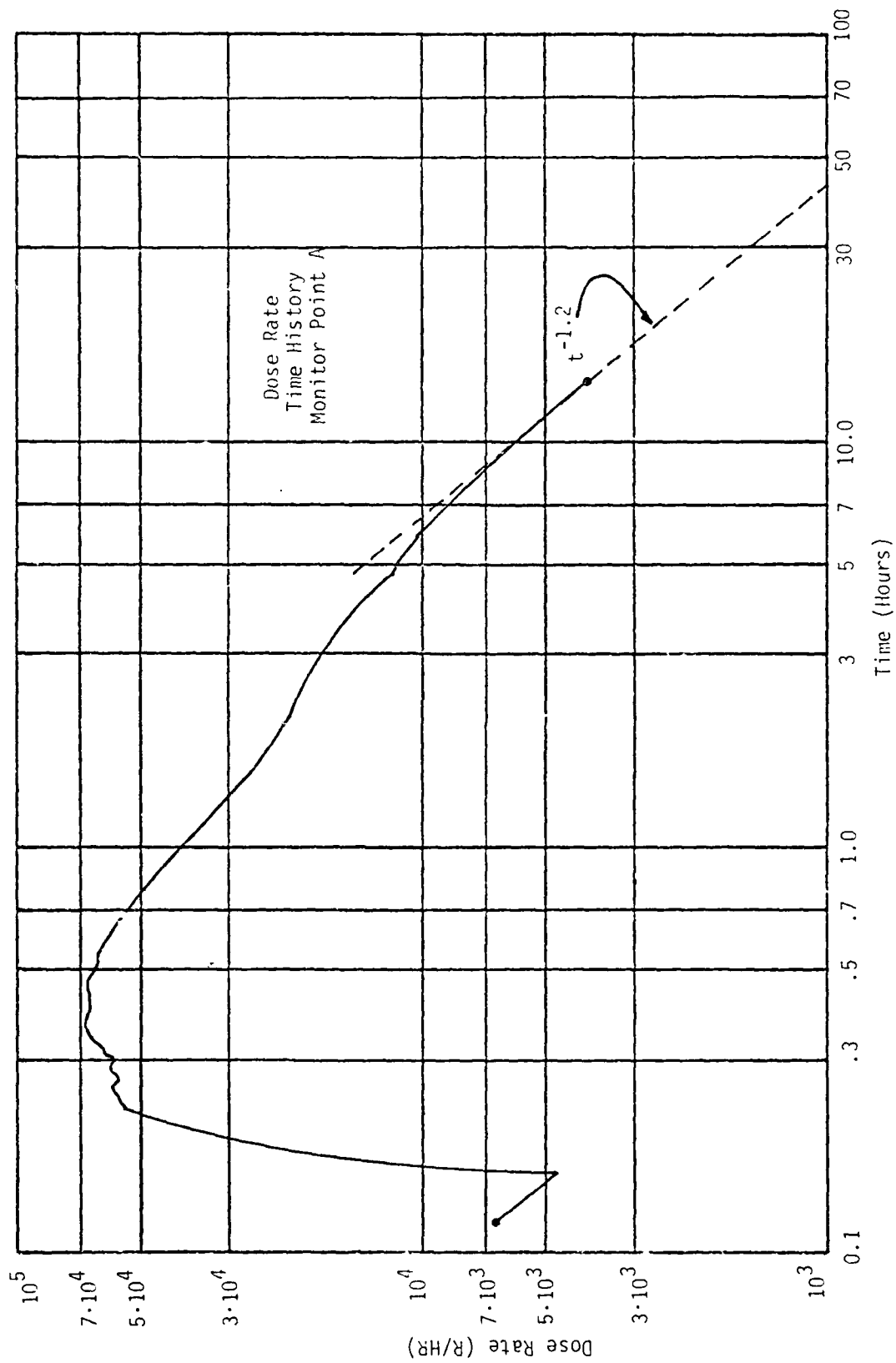


Figure 5.9 Dose Rate Time History, Monitor Point A

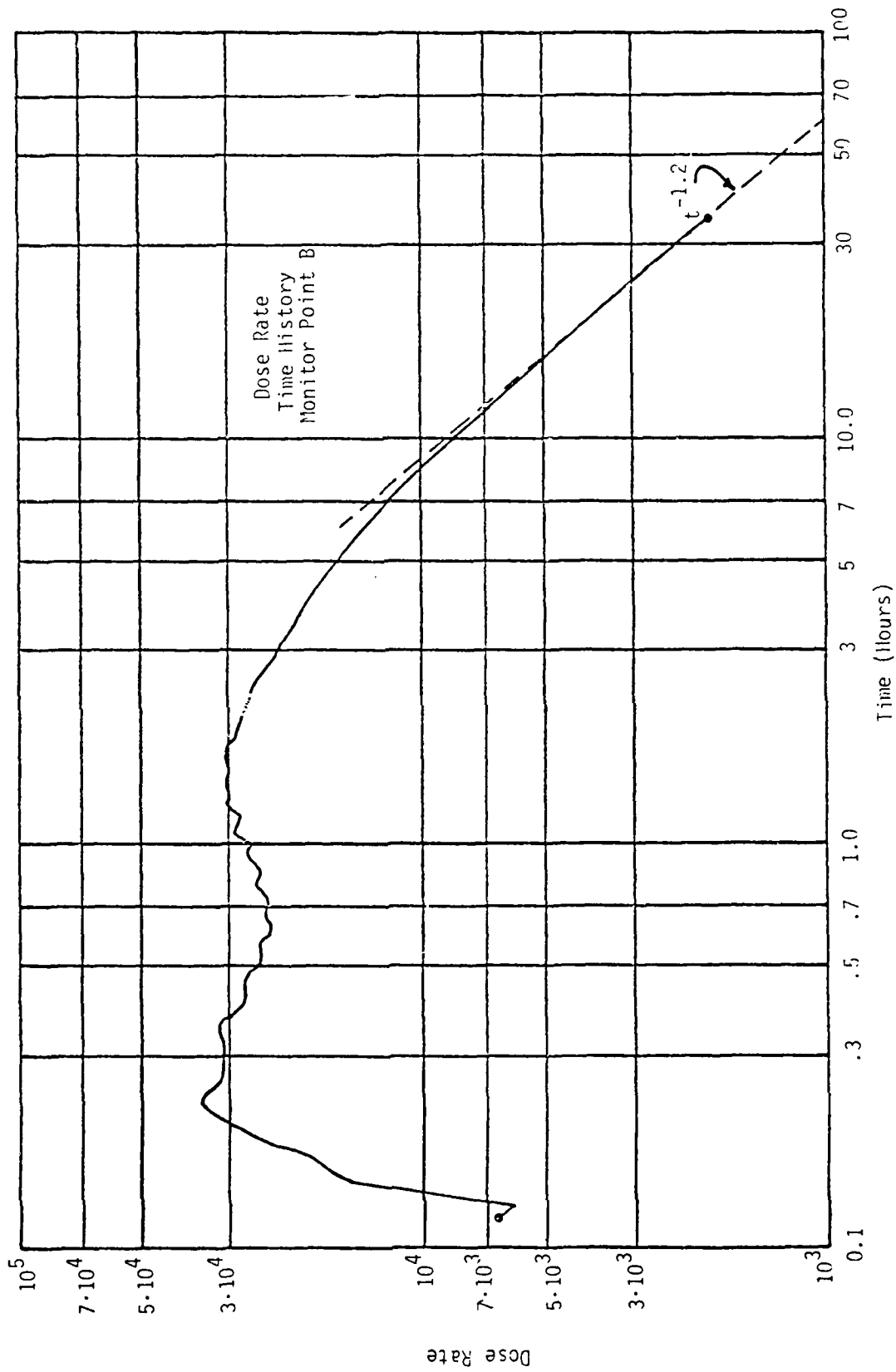


Figure 5.10 Dose Rate Time History, Monitor Point B

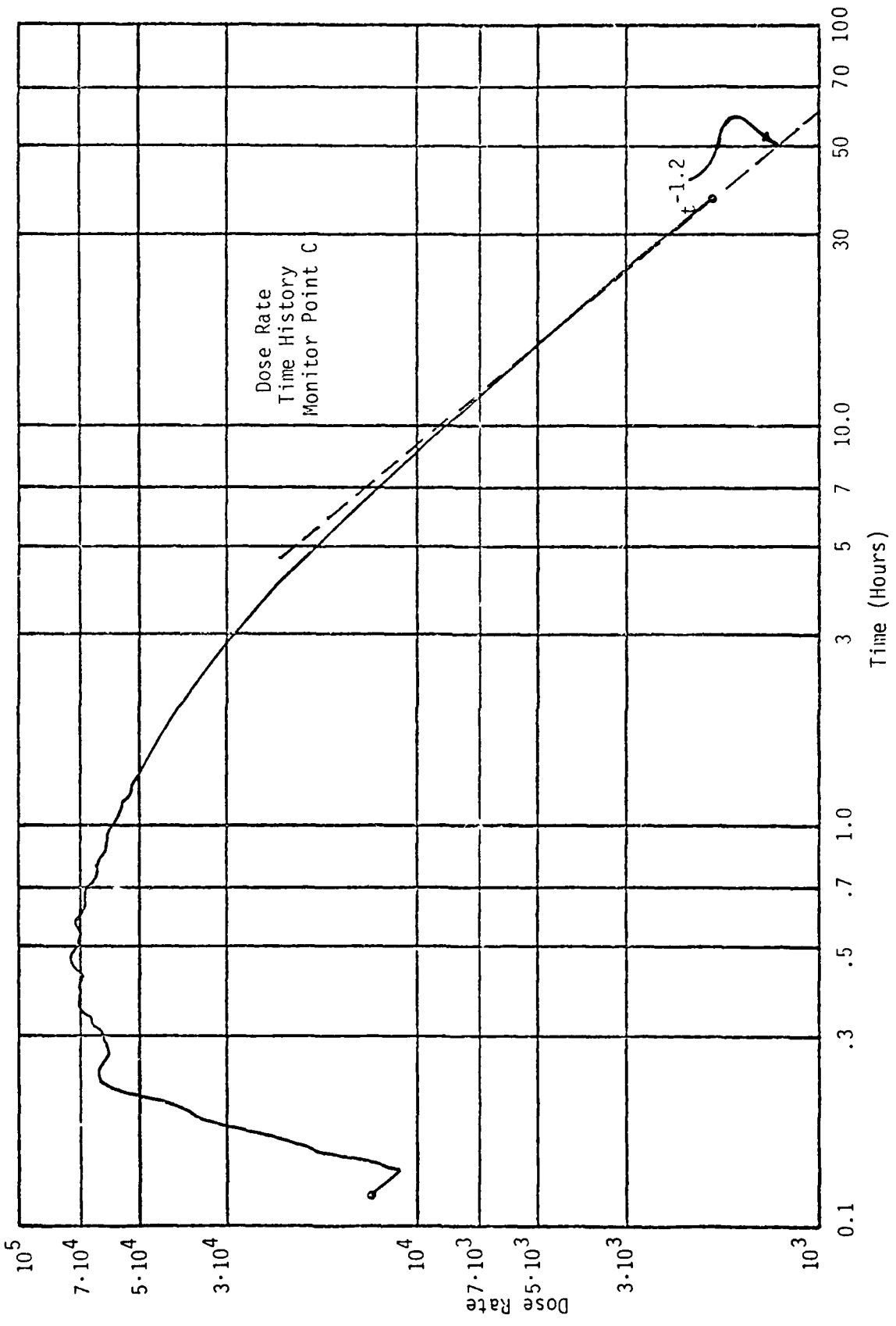


Figure 5.11 Dose Rate Time History, Monitor Point C

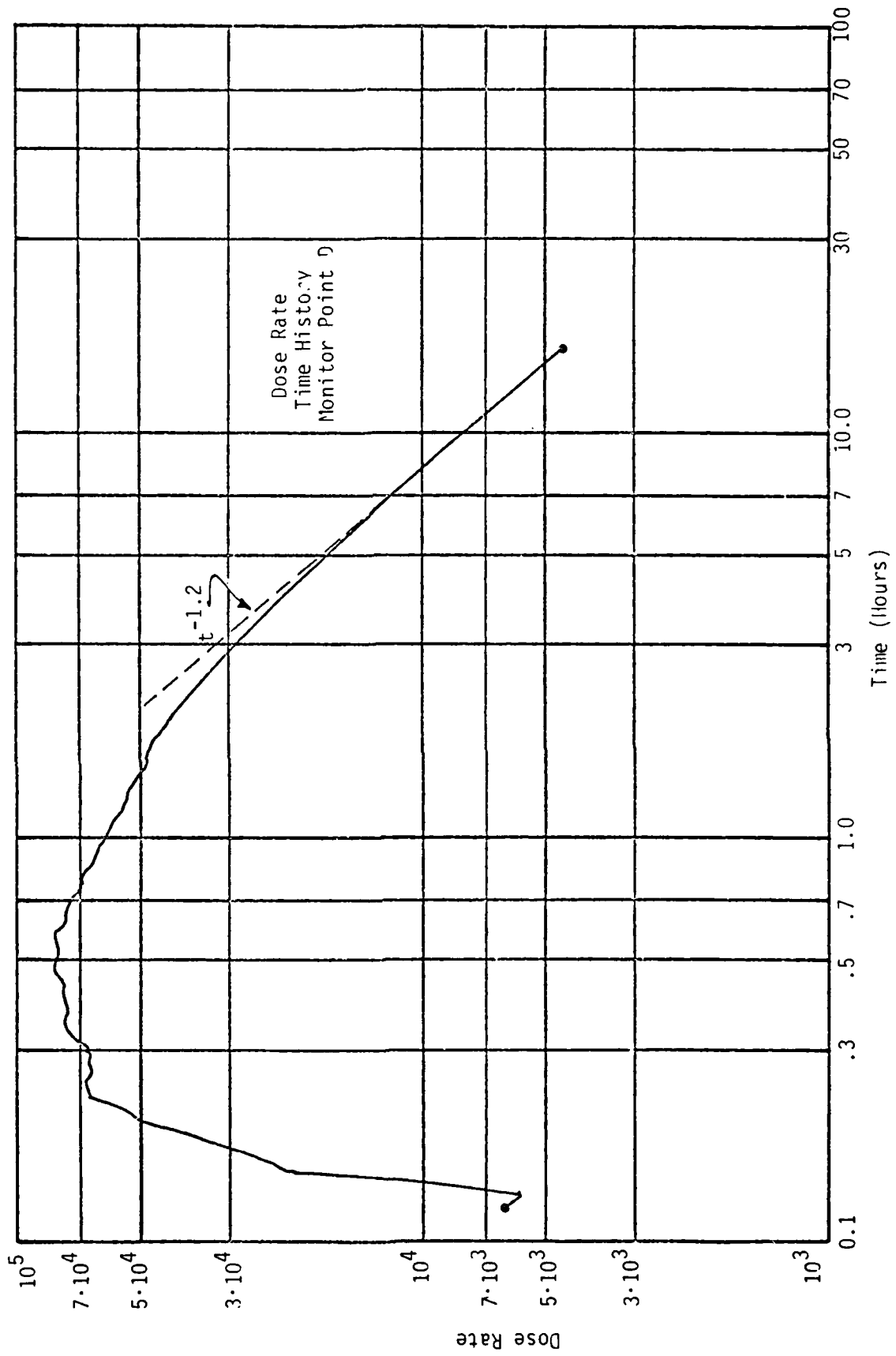


Figure 5.12 Dose Rate Time History, Monitor Point D

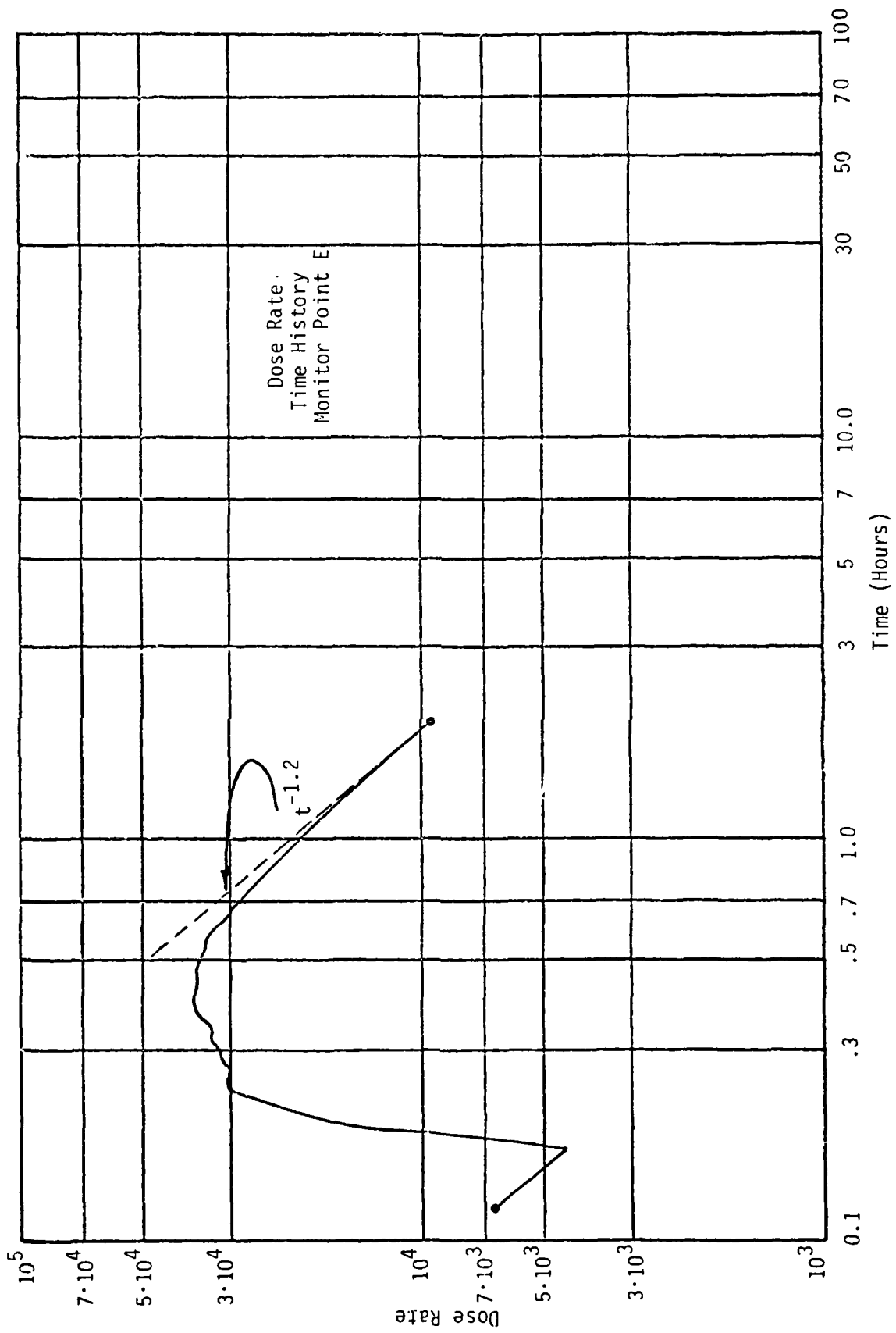


Figure 5.13 Dose Rate Time History, Monitor Point E

SECTION 6

REFERENCES

1. "The Effects of Nuclear Weapons," Third Edition, U.S. Departments of Defense and Energy, U.S. Government Printing Office, 1977.
2. "Department of Defense Land Fallout Prediction System, Vol. I-Vol. VI," DASA 1800-I through VI, Technical Operations Research, Burlington, Mass., June 1966.
3. "Guide to Standard Weather Summaries and Climatic Services," NAVAIR 50-1C-534, NWSED Asheville, January 1973.
4. J. Wesley Miller, et al., "Modeling of Multiple Burst Dust and Ice Environments," Science Applications, Inc. (Unpublished)
5. C. Needham and L. Wittwer, "Air Force Weapons Laboratory Low Altitude Multiburst (LAMB) Model," AFWL-DYT-TN-75-2 (unpublished).
6. B. Chambers, "Modeling Multiburst Dust Clouds," Science Applications, Inc., SAI-79-702-AQ, October 1978.
7. Mark A. Fry, et al., "The HULL Hydrodynamics Computer Code," AFWL-TR-76-183, Air Force Weapons Laboratory, September 1976.
8. R. Clemens and D. Matuska, "Air Force Weapons Laboratory Hydrodynamic Calculations in Two- and Three-Dimensions," Air Force Weapons Laboratory. (Unpublished)

APPENDIX A
ABBREVIATIONS

A	Area
BPX_j	X coordinate of a Burst Point
BPY_j	Y coordinate of a Burst Point
D	Dose Rate
DELFIIC	Department of Defense Land Fallout Prediction System
D_{BP_j}	Dose Rate due to Burst Point j
D_{MP_i}	Dose Rate at Monitor Point i
D_{PMP_j}	Dose Rate at Pseudo Monitor Point j
DR_1	Dose Rate at H+1 Hour
FF	Fission Fraction
ICBM	Intercontinental Ballistic Missile
K	K-Factor
m	Number of Monitor Points or Size Classes
MPS	Multiple Protective Structure
MPY_i	Y coordinate of an Actual Monitor Point
MPX_i	X coordinate of an Actual Monitor Point
MT	Megaton
MX	Missile Experimental
n	Number of Burst Points or Cloud Wafers
$PMPX_{i,j}$	X coordinate of n Pseudomonitor Points for each of the m Actual Monitor Points
$PMPY_{i,j}$	Y coordinate of n Pseudomonitor Points for each of the m Actual Monitor Points
R_{MAX}	Maximum Cloud Radius
R_c	Radius of Cloud
\vec{R}_j	A Vector from Burst Points to Monitor Points
R/HR	Roentgens/Hour
RAD	Radiation Absorbed Dose
S_j	A Vector from a Reference Burst Point to a Pseudo Monitor Point

S_j

A vector from a Reference Burst Point
to a Pseudomonitor Point

SPO

Special Project Office

W

Weapon Yield

DISTRIBUTION LIST

DEPARTMENT OF DEFENSE

Armed Forces Radiobiology Research Institute
ATTN: Director

Assistant Secretary of Defense
International Security Affairs
ATTN: Policy Plans & NSC Affairs
ATTN: ISA/PF
ATTN: J. Kaufman
ATTN: D. Alderson

Assistant Secretary of Defense
Program Analysis & Evaluation
ATTN: Strategic Programs
ATTN: S. Sienkiewicz

Assistant to the Secretary of Defense
Atomic Energy
ATTN: L. Michael
ATTN: Executive Assistant
ATTN: Strategy & Assessment
ATTN: T. Sisson
ATTN: Nuclear Policy Planning

Defense Advanced Rsch. Proj. Agency
ATTN: TIO
ATTN: TTO

Defense Intelligence Agency
ATTN: DN
ATTN: DB-1, F. Walker
ATTN: DB-4D, H. Ward
ATTN: RDS-3C
ATTN: DIO-GPF, W. Magathan
ATTN: DT, J. Vorona
ATTN: DIR 4

Defense Nuclear Agency
ATTN: DDST
ATTN: VLWS
ATTN: SPAS
ATTN: STVL
ATTN: STSP
2 cy ATTN: RATN
4 cy ATTN: TITL

Defense Technical Information Center
12 cy ATTN: DD

Field Command
Defense Nuclear Agency
ATTN: FCPR
ATTN: FCP, J. DiGrazia

Field Command
Defense Nuclear Agency
Livermore Division
ATTN: FCPRL

Field Command
Defense Nuclear Agency
Los Alamos Branch
ATTN: FCPRA

Interservice Nuclear Weapons School
ATTN: Document Control

DEPARTMENT OF DEFENSE (Continued)

Joint Chiefs of Staff
ATTN: SAGA/SFD
ATTN: J-5
ATTN: SAGA/SSD
ATTN: J-3

Joint Strat. Tgt. Planning Staff
ATTN: JSTPS/JLA, R. Haag
ATTN: JPS
ATTN: JLTW
ATTN: JL
ATTN: JP

Undersecretary of Defense for Rsch. & Engrg.
ATTN: Strategic & Space Systems (OS)

DEPARTMENT OF THE ARMY

Harry Diamond Laboratories
Department of the Army
ATTN: DELHD-N-P

U.S. Army Air Defense School
ATTN: COL Rinehart

U.S. Army Ballistic Research Labs.
2 cy ATTN: DRDAR-BLB, J. Maloney

U.S. Army Missile Command
ATTN: DRCPM-PE, W. Jann
ATTN: DRSMI-YDR
ATTN: DRDMI-EAA, E. Harwell

DEPARTMENT OF THE NAVY

Anti-Submarine Warfare Sys. Proj. Ofc.
Department of the Navy
ATTN: PM-4

Center for Naval Analysis
ATTN: NAVWAG

Naval Academy
ATTN: Nimitz Library/Technical Rpts. Branch

Naval Surface Weapons Center
ATTN: Code F31

Naval War College
ATTN: Code E-11

Naval Weapons Evaluation Facility
ATTN: Technical Director
ATTN: G. Binns

Office of Naval Research
ATTN: Code 200
ATTN: Code 431

DEPARTMENT OF THE AIR FORCE

Air Force School of Aerospace Medicine
ATTN: Radiobiology Division

DEPARTMENT OF THE AIR FORCE (Continued)

Air Force Weapons Laboratory
Air Force Systems Command
ATTN: DYT
ATTN: NSSB
ATTN: SUL

Air Weather Service, MAC
Department of the Air Force
ATTN: AWSAE

Assistant Chief of Staff
Intelligence
Department of the Air Force
ATTN: INE

Assistant Chief of Staff
Studies & Analyses
Department of the Air Force
ATTN: AF/SAMI
ATTN: AF/SAGF

Deputy Chief of Staff
Operations Plans and Readiness
Department of the Air Force
ATTN: AFXOXM
ATTN: AFXOFT
ATTN: AFXOOR
ATTN: Director of Plans
ATTN: Director of Operations & Plans
ATTN: AFXOOTR

Deputy Chief of Staff
Research, Development, & Acq.
Department of the Air Force
ATTN: AFRDQSM
ATTN: AFRDQR

Tactical Air Command
Department of the Air Force
ATTN: DO
ATTN: DRA
ATTN: XP
ATTN: XPB
ATTN: INO
ATTN: DR

DEPARTMENT OF ENERGY

Department of Energy
ATTN: Document Control for EV, H. Hollister

DEPARTMENT OF ENERGY CONTRACTORS

Sandia Laboratories
ATTN: Document Control for 3141
ATTN: Document Control for J. Kaizur

DEPARTMENT OF ENERGY CONTRACTORS (Continued)

Sandia Laboratories
Livermore Laboratory
ATTN: Document Control for T. Gold

OTHER GOVERNMENT AGENCIES

Central Intelligence Agency
ATTN: OSR/SE/F, A. Rehm
ATTN: OSI/NED
ATTN: OSR/SEC

Federal Emergency Management Agency
ATTN: Postattack Research Division
ATTN: Asst. Dir. for Rsch., J. Buchanon
ATTN: D. Benson
ATTN: G. Sisson
ATTN: C. McLain

U.S. Arms Control & Disarmament Agency
ATTN: A. Lieberman
ATTN: C. Thorn
ATTN: Ops. & Analysis Div., W. Deemer

DEPARTMENT OF DEFENSE CONTRACTORS

Academy for Interscience Methodology
ATTN: N. Pointer

Boeing Co.
ATTN: L. Harding

Decision-Science Applications, Inc.
ATTN: Dr. Galiano

General Electric Company-TEMPO
ATTN: DASIAC

General Electric Company-TEMPO
ATTN: DASIAC

Pacific-Sierra Research Corp.
ATTN: H. Brode

R & D Associates
ATTN: C. MacDonald

Science Applications, Inc.
ATTN: M. Drake
ATTN: J. Martin

Science Applications, Inc.
ATTN: J. Goldstein
ATTN: W. Layson
ATTN: J. McGahan
ATTN: R. Craver
ATTN: E. Muller